

# e-Newsletter n°4

November 2008

Available at <http://www.ist-brighter.eu>

---



## WWW.BRIGHTER.EU

### *World Wide Welfare: High-Brightness Semiconductor Lasers for Generic Use*

WWW.BRIGHTER.EU is an integrated project supported by the European Commission's Information Society Technologies programme

#### CONTENT

Greetings from the Project Coordinator	2
<b>PROJECT NEWS</b>	
Latest Achievements	3
Partner Presentations	7
<b>APPLICATIONS TOPICS</b>	
Recent Progress in Interstitial Photodynamic Therapy for Solid Tumors	11
External Cavity Lasers: Recent Developments within BRIGHTER	16
<b>TECHNICAL TOPICS</b>	
Mirror Heating in High Power Lasers	26
High-Brightness Tapered Lasers with Multiple Contacts	31
<b>DISSEMINATION &amp; OUTREACH</b>	
NUSOD 2008 Conference	40
High Power Diode Lasers and Systems Meeting	41
RichMedia CDs and Project Website	42
Selected Publications and Presentations	44
Next e-Newsletter & Back Issues	45
Calendar of Events	46
BRIGHTER at ICT 2008	46

---

**Legal Note:** The contents of this newsletter are the property of their respective authors. Reproduction of the contents in whole or part is forbidden without the express written consent of the authors.

## EDITORIAL

Welcome to the 4<sup>th</sup> e-Newsletter of the 3 year integrated project WWW.BRIGHTER.EU, which began in October 2006. This integrated project builds upon the earlier WWW.BRIGHT.EU project, in which we published our first series of e-Newsletters.

If you missed either of the previous three editions of our e-Newsletter, then please visit our website to download your copy. The next e-Newsletter will be published in March 2009.

We hope you will enjoy reading this e-Newsletter and learning about the latest developments in our project.

*The Editors*



*Steve Bull*  
University of Nottingham  
[steve.bull@nottingham.ac.uk](mailto:steve.bull@nottingham.ac.uk)



*Myriam Oudart*  
Alcatel Thales III-V lab  
[myriam.oudart@3-5lab.fr](mailto:myriam.oudart@3-5lab.fr)



*Eric Larkins*  
University of Nottingham  
[eric.larkins@nottingham.ac.uk](mailto:eric.larkins@nottingham.ac.uk)

## GREETINGS FROM THE PROJECT COORDINATOR

Dear Reader,

Welcome to the fourth e-Newsletter of our EC-IST Project *World Wide Welfare: High-Brightness Semiconductor Lasers for Generic Use (WWW.BRIGHTER.EU)*, an Integrated Project on high-brightness laser diode technologies and applications, which began in October 2006.



*Michel Krakowski*  
Project Coordinator  
Alcatel Thales III-V Lab  
[michel.krakowski@3-5lab.fr](mailto:michel.krakowski@3-5lab.fr)

Since our last e-Newsletter, we've reached the two year mark in our project and have again had some great successes. The project is well on schedule and we have an exciting final year ahead of us. We have continued to work not only on the technical objectives, but also on our training and project outreach activities. If you've not checked out our project website, [www.ist-brighter.eu](http://www.ist-brighter.eu), recently then I encourage you to visit soon and browse the wide range of new materials that have been added. The Consortium are also working hard to put on an exciting display at the forthcoming ICT Event in Lyon. Here, you'll be able to look at devices, modules and systems developed within the project, talk to members of the team and learn more about all aspects of this project. We look forward to welcoming you to our booth.

Inside this e-Newsletter, you will find an update on some of our latest technical achievements followed by profiles of four more project partners. There are also four extended articles in this e-Newsletter. Two applications topics cover interstitial PDT and recent developments in the field of external cavity lasers. Technical papers are presented on mirror heating in high-power lasers and high-brightness lasers with multi-contacts. There is also a report on the NUSOD 2008 Conference, which was hosted by a BRIGHTER partner, the University of Nottingham. Details are also given about the latest changes to our project website and our RichMedia CD format, which we are using to distribute technical tutorials and workshop presentations to the wider scientific and educational community. At the end of this edition, you can find details of some of our recent publications, a calendar of forthcoming events, a preview of the next e-Newsletter and details of where to find BRIGHTER at the European Commissions' forthcoming ICT Event to be held in Lyon towards the end of this month.

*Michel Krakowski*

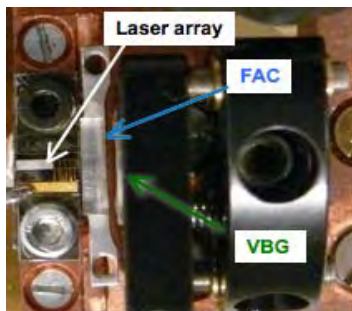
## TECHNICAL ACHIEVEMENTS Towards the Project Objectives

The WWW.BRIGHTER.EU Project Consortium continues to be successful across the broad range of areas in the project. Here, we present the latest news and briefly review some of the recent and most exciting highlights ranging from a new green laser for display applications and a novel external cavity scheme for phase-locking and wavelength stabilisation to laser modelling and comparisons of simulated designs with experimental results.

### Novel concurrent phase-locking and wavelength stabilisation of a tapered laser array

LCFIO has demonstrated the concurrent phase-locking and wavelength stabilisation of an array of index-guided tapered lasers in a novel external cavity configuration with a volume Bragg grating as the output coupler. The coherent emission of the array is based on the Talbot self-imaging effect, which is responsible for the phase-coupling between the emitters in the external cavity. The laser bar was manufactured at III-V Lab. In a compact and stable prototype, the output power reaches 1.7 W in a single-mode of operation from a bar of 10 independent lasers. Furthermore, the full spectrum is locked to the Bragg wavelength within 0.1 nm, independent of the operating conditions.

This design should lead to improvements in the brightness of semiconductor laser arrays and widen their application range. (For more details, see the Applications Article on External Cavity Lasers starting on Page 16 of this edition.)



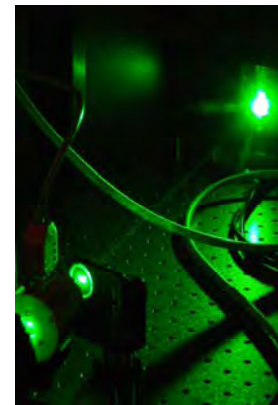
Photograph showing the compactness of the experimental prototype (VBG – Volume Bragg Grating, FAC – Fast Axis Collimator).

### High-power green laser for display applications

DTU Fotonik have demonstrated a compact and robust high-power green laser system based on an infrared diode laser and second harmonic generation (SHG).

More than 450 mW of output power at a wavelength of 531 nm has been achieved by single-pass SHG of a 1062 nm high-power multi-section DBR tapered laser, fabricated by FBH.

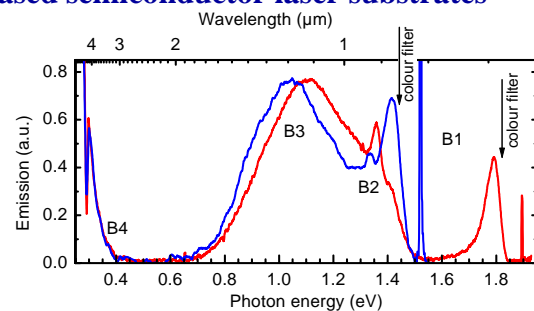
By modulating the current to the ridge section of the laser, it is possible to modulate the green light at high speed making it ideal as a compact, robust, and efficient green light source for display applications.



### Observation of near-IR emission from GaAs-based semiconductor laser substrates

In work at MBI, we have observed and revealed the origins of three additional low-energy spontaneously emitted bands in GaAs-based broad-area laser diodes supplied by partners FBH and OSRAM. Spectrally- and spatially-resolved scanning optical microscopy and Fourier-transform infrared spectroscopy assign these contributions to bandtail related luminescence from the gain region as well as interband and deep level related luminescence from the GaAs substrate. The latter processes are photo-excited due to spontaneous emission from the active region followed by a cascade-like photon-recycling process within the substrate.

M. Ziegler et al., *Applied Physics Letters*, Vol. 93, 041101, July 2008.

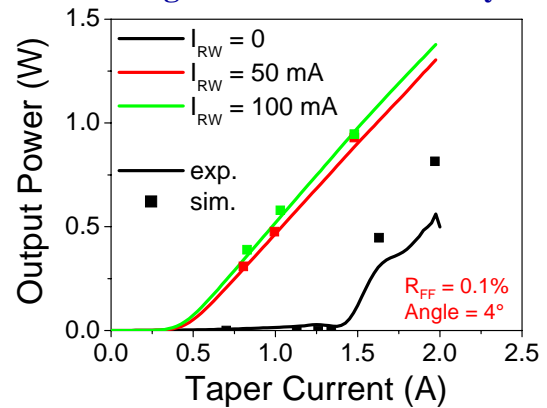


Emission spectra of a red-emitting device (red line,  $I = 0.7$  A, heatsink temperature  $T = 23$  °C) and a NIR device (blue line,  $I = 1.9$  A,  $T = 50$  °C). The absorption edges of long pass colour filters at 690 and 850 nm and of GaAs are indicated by arrows.

## TECHNICAL ACHIEVEMENTS Towards the Project Objectives

### Design of separated-contact 1060 nm tapered lasers with high modulation efficiency

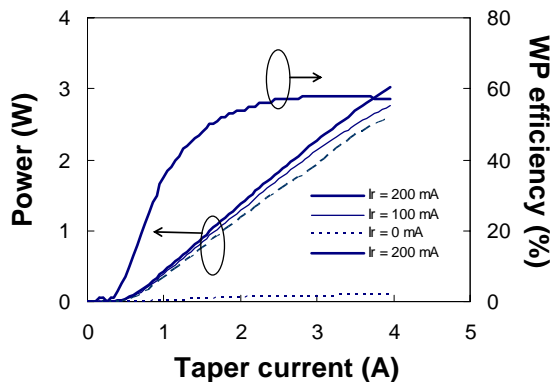
Tapered lasers with separated contacts were simulated, by the University of Madrid, prior to fabrication with the goal of increasing the modulation efficiency (the ratio of the change in the output power when the current in the ridge waveguide section is changed). The simulation predicted that a high modulation efficiency could be achieved by decreasing the front facet reflectivity. The figure opposite compares the simulation predictions with the experimental power-current characteristic of a 4° tapered laser fabricated by III-V Lab and shows excellent agreement. A record value of modulation efficiency (50 W/A) was measured in devices with a taper angle of 6°.



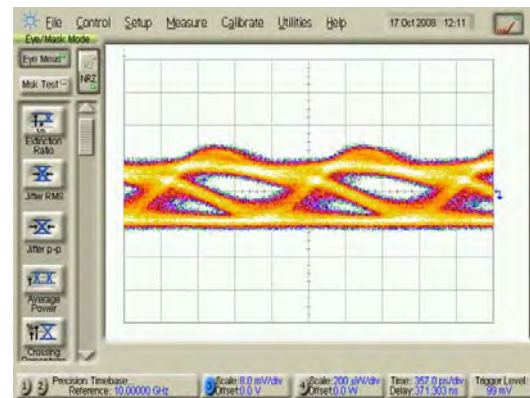
### Two-electrode high-brightness tapered laser for optical wireless & display applications

Two-electrode high-brightness tapered lasers with separate excitation for a modulating and a constant drive current are being investigated to obtain simultaneous high power and high modulation speed operation. The separate excitation allows a small input signal current swing to achieve a high modulation depth for the output optical power using existing standard optical communication components.

On a gain-guided two-electrode tapered laser at 1060 nm, realised by III-V Lab and designed in cooperation with the University of Madrid (see above), we have obtained a high CW power of 3 W at 10 °C, together with a good beam quality ( $M^2 = 3.7$ ). In the static regime, at the fixed taper current of 4 A, the laser has a very large modulation efficiency – the power moves from 90 mW when the ridge current is 0 mA to 2.6 W when the ridge current is 50 mA.



*High-power tapered laser at 1060 nm (static regime).*



*Eye diagram at 700 Mbps, 1.7 W modulated optical power at a ridge current of 84 mA (20 W/A).*

In collaboration with the University of Cambridge, we have obtained a very high modulated optical power of 1.7 W for a small modulation current of 84 mA at 700 Mbps. This corresponds to a high modulation efficiency of more than 20 W/A. The optical extinction ratio is also very high with a value of 21 dB.

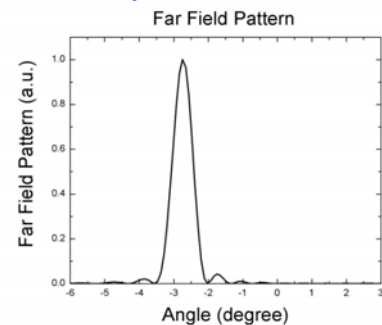
The combination of high speed, high extinction ratio, high power, high brightness and high modulation efficiency make these devices very interesting for free-space optical wireless communications and laser display applications.

## TECHNICAL ACHIEVEMENTS Towards the Project Objectives

### Predictive modelling of an external cavity broad-area laser with asymmetric feedback

A model of a broad-area laser diode which is operating in an external cavity with asymmetric feedback has been developed by the University of Nottingham. The model consists of a steady-state model of the laser, which has antireflection coatings on both facets, and a model of the optical propagation through the bulk optical elements in the external feedback path. The simulations predict the laterally-shifted narrow far-field pattern that has been experimentally observed by DTU Fotonik. For more details, see the article on External Cavity Lasers on Page 16.

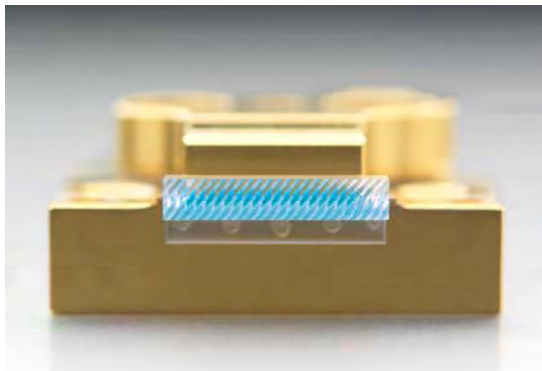
*L. Lang et al., "Improvement of the Beam Quality of a Broad Area Diode Laser using Asymmetric Feedback from an External Cavity", NUSOD 2008, Nottingham, Sept. 08.*



### New FISBA Beam Twister™ FBT based on 200 micron diode laser pitch

FISBA OPTIK AG has extended its range of micro-optic components for beam symmetrisation. The FISBA Beam Twister FBT 200 is made up of a Fast Axis Collimation lens (FAC) and the patented beam twister element. Now, diode laser arrays with a 200 micron pitch and a maximum emitter width of 80 microns can be optimally symmetrised and subsequently coupled into a fibre with a special focussing optical system. First prototypes built for a specific application show a coupling efficiency of 70% into a 100 micron fibre.

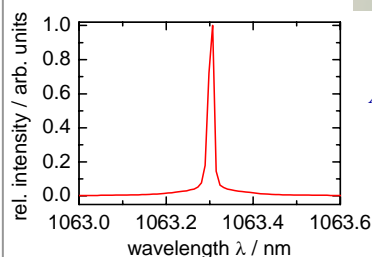
The FBT 200 element is available for visible and close to infrared wavelengths. The existing design covers diode arrays with up to 20 emitters. Flexible production processes allow it to be adjusted and optimised to other diode specifications.



### High-brightness 1060 nm diode lasers

Ferdinand-Braun-Institut für Höchstfrequenztechnik have realised high-brightness 1060 nm monolithic diode lasers, which are suitable for the efficient generation of more than 1 W of green light via second harmonic generation. The output power of the NIR diode laser exceeds 10 W. The spectral width is well below 50 pm (see figure), even under modulation conditions. The beam propagation ratio of the central lobe containing more than 75% of the power is about 1.2. The lateral and vertical divergences are quite low at 13° and 15°, respectively. The device is a so-called DBR tapered laser consisting of two sections with separate electrical contacts and a grating section providing spectral stability and narrow linewidth. The grating and one contact are implemented in a narrow single mode waveguide region. The second contact has a tapered geometry. The process is relatively simple and thus suitable for mass production. The technology is based on standard processing steps, including deep etching of a higher order grating, with a period of only about 1 µm.

*Below: Spectrum of the 1060 nm DBR tapered laser at P = 10 W, T = 25°C and I<sub>rw</sub> = 300 mA.*



*Above: Photograph of a mounted dual contact DBR tapered laser.*

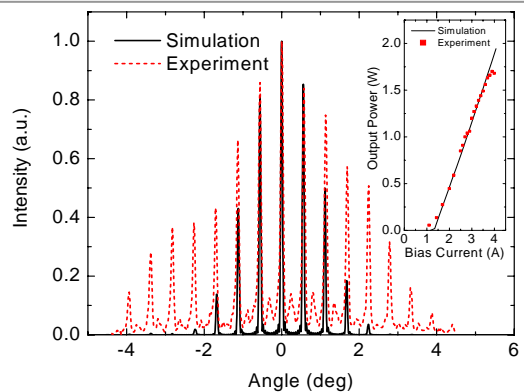
## TECHNICAL ACHIEVEMENTS Towards the Project Objectives

### Array phase coupling using the Talbot effect

The University of Nottingham and LCFIO are breaking new ground on the design and modelling of external cavity lasers to improve the beam brightness, using both external Talbot cavities and self-organising laser cavities based on photo-refractive crystals. These simulations are being performed in close coordination with experimental investigations and the first results are very promising. For example, the phase coupling of the laser diode emitters using the Talbot effect has been demonstrated as shown opposite. The initial simulation results for self-organising cavity lasers are also promising. More information on these and other external cavity laser results can be found in the article on Page 16.

*D. Paboeuf et al., "Numerical and experimental study of a high-power narrow-line phase-locked tapered laser array in an external cavity," accepted for oral presentation at Advanced Solid State Photonics, February 2009.*

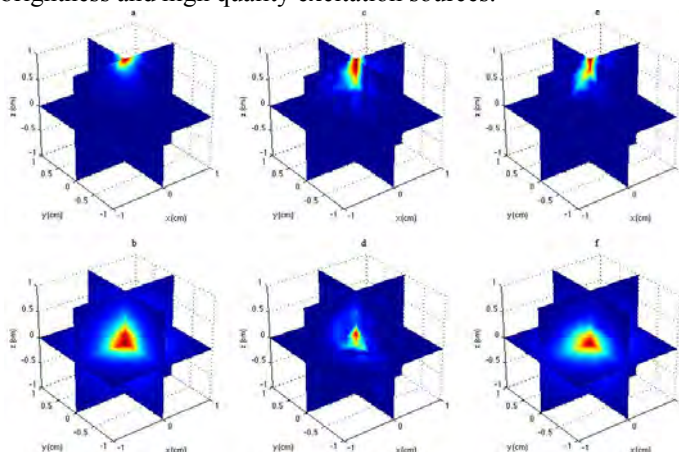
*J.J. Lim et al., "Design and simulation of next-generation high-power, high-brightness laser diodes," (invited) submitted to Journal of Selected Topics in Quantum Electronics, November 2008.*



*Simulated and experimental results for a phase-coupled array employing an external Talbot cavity*

### A coupled radiative transfer & diffusion approximation model for solving the forward problem and *a priori* estimation of fluorophore distribution in fluorescence imaging

The Institute of Communications and Computer Systems at the National Technical University of Athens has developed a coupled radiative transfer (RTE) and diffusion approximation (DA) model for fluorescence molecular imaging. The forward solver utilises the accuracy of the radiative transfer equation and the time efficacy of the diffusion approximation and is solved in 3D-space. For the first time, the solver introduces super-ellipsoid models and sophisticated image-processing algorithms to also provide an *a priori* estimation of the fluorophore distribution – information that is very important for the solution of the inverse problem. Simulations have proven that this method presents extensive success on the registration between acquired and simulated images, under the premise that the fluorescence molecular imaging system is based on high brightness and high quality excitation sources.



*Photon density magnitude for the emission (top) and the excitation (bottom) fields from the DA model (a, b), the RTE model (c, d) and the coupled RTE-DA model (e, f) plotted as 2D slices with respect to the entire 3D region.*

*D. Gorpas, K. Politopoulos and D. Yova, to be presented at Multimodal Biomedical Imaging IV, Photonics West, BIOS 09, San Jose, CA, USA (2009).*

### BRIGHTER reaches out more

The BRIGHTER project continues to reach out to students and the wider scientific world through its project website, which has seen many new additions over recent months. More than ten video-recorded tutorials and workshop presentations can now be downloaded or streamed online. These materials are free to access and may be used as teaching materials or for independent learning. Over the next year, the number of tutorials that are available online will double. More details can be found on pages 42-43.

*Visit [www.ist-brighter.eu](http://www.ist-brighter.eu) now*

## PARTNER PRESENTATIONS

In this section of the e-Newsletter, we introduce some of the partners in the project Consortium. In this edition, profiles are presented for the Centre National de la Recherche Scientifique – Laboratoire Charles Fabry de l'Institut d'Optique, Universidad Politécnica de Madrid, Ferdinand-Braun-Institut für Höchstfrequenztechnik and DTU Fotonik (formerly Risø National Laboratory).

### Centre National de la Recherche Scientifique - Laboratoire Charles Fabry de l'Institut d'Optique

The Centre National de la Recherche Scientifique (CNRS, National Centre for Scientific Research) is the largest fundamental research organisation in Europe. It is a government-funded research organisation under the administrative authority of France's Ministry of Research. Founded in 1939, the CNRS carries on its activities in all the fields of knowledge, from mathematics to high-energy physics, environmental sciences as well as humanities and social sciences. CNRS encourages collaboration between specialists from different disciplines in particular with the university thus opening up new fields of enquiry to meet social and economic needs. CNRS research units are located throughout France, and employ a large body of tenured researchers, engineers, and support staff. CNRS's annual budget represents a quarter of French public spending on civilian research.



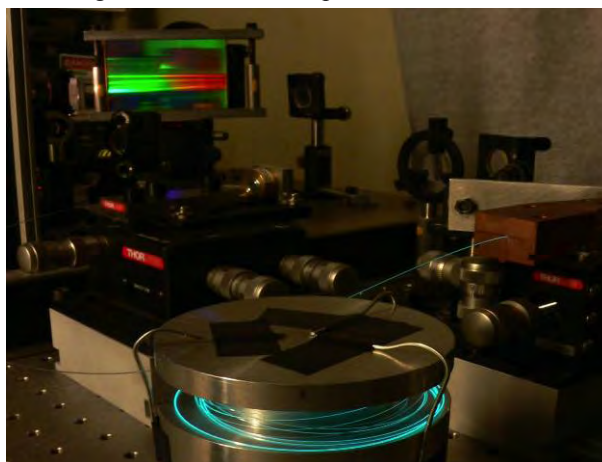
*The Institut d'Optique in Palaiseau (France).*

The Laboratoire Charles Fabry de l'Institut d'Optique (LCFIO) is a joint laboratory partnered with CNRS and the Institut d'Optique, in cooperation with the Université Paris-Sud XI. It covers a broad range of optical research, both fundamental and applied, with emphasis on experimental aspects.

Skills covering essentially all of optics are highlighted by the timely research topics conducted by the six research groups:

- Atom Optics
- Quantum Optics
- Nanophotonics and Electromagnetism
- Optical Components and Systems
- Lasers and Biophotonics
- Non-linear Materials and Applications

The institute presently has about 100 members of staff, including 50 PhD students & post-doctoral researchers.



*High-power diode-pumped fibre chirped-pulse amplifier under femtosecond operation.*

### Activities within WWW.BRIGHTER.EU

The Lasers and Biophotonics and Non-linear Materials and Applications groups are both involved in the BRIGHTER project, mainly in Workpackage 3 dealing with External Cavity Lasers. LCFIO works on high-brightness extended cavity designs for the wavelength stabilisation of single-emitter lasers and laser bars. Furthermore, LCFIO investigates, both theoretically and experimentally, novel architectures for the improvement of the spatial quality of laser bars, based on the coherent combining of laser emitters within an external cavity. Additionally, LCFIO is responsible for the spectral improvement of laser diodes using self-organising laser cavities, and is in charge of the modelling of the self-organising operation resulting from the introduction of a photorefractive crystal in an extended cavity. This modelling is carried out in close collaboration with the University of Nottingham.

### Further Information

Further information can be obtained from:

Dr. Gaëlle Lucas-Leclin

Email: [gaelle.lucas-leclin@institutoptique.fr](mailto:gaelle.lucas-leclin@institutoptique.fr)

Web: <http://www.cnrs.fr>, <http://www.institutoptique.fr>

## Universidad Politécnica de Madrid

The **Universidad Politécnica de Madrid (UPM)**, the Technical University of Madrid, is the largest academic institution in Spain devoted to education and research in engineering and applied sciences. It has more than 4000 faculty personnel and PhD students who participate in research and development projects funded by local, national and European institutions, both public and private. Since 1998, UPM is one of the most active European institutions in the EU Framework Programs: it has participated in 143 projects of FP6 with a total funding of around 25M€. In 2006, the total annual income in R&D activities amounted to more than 100M€, 65% of which was obtained in cooperation with the industrial sector.

UPM is participating in WWW.BRIGHTER.EU through the “Grupo de Fotónica Aplicada (GFA)” (Applied Photonic Group) at the “Departamento de Tecnología Fotónica” (Photonic Technology Department). The GFA is involved in several European, national and local government projects related to photonic devices and systems for a wide range of applications, including liquid crystal displays and modulators, qualification of photonic components for space applications, wireless optical communications for space and domestic applications and modelling, design and characterisation of laser diodes.

The activities of GFA in semiconductor lasers started in 1992 and since then it has participated in different European (“NODELASE” 1996-99, “ULTRABRIGHT”, 2000-03, “WWW.BRIGHTER.EU”, 2004-06) and national projects in collaboration with international and national groups. The main research fields of the group in recent years have been: modelling of high speed laser dynamics, including carrier capture and escape balance, new techniques for laser diode characterisation (capacitance-voltage, sub-threshold power-current-voltage, gain and linewidth enhancement factor measurements and spatially resolved spectral analysis), modelling of high-brightness tapered lasers, and the modelling and applications of VCSELs. The group has published more than 100 journal and conference papers on laser diodes, and has developed and registered a software program for the simulation of high power lasers (HAROLD 3.0), which is currently under commercial exploitation.

### Activities within WWW.BRIGHTER.EU

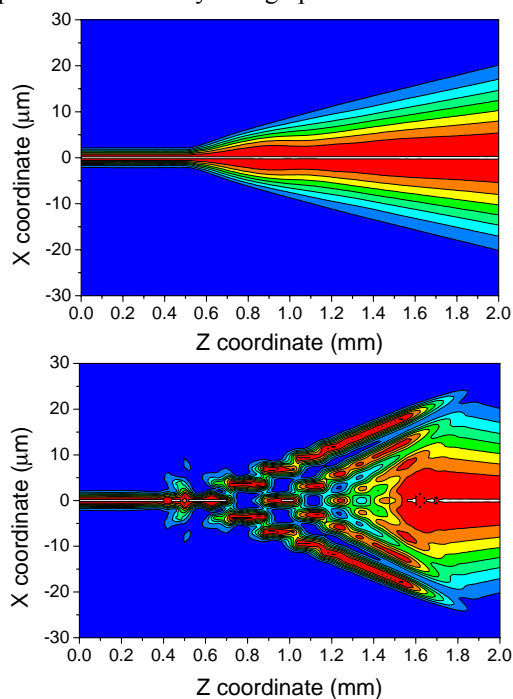
UPM contributes to the project in the area of modelling, simulation and design of high brightness and high wall-plug-efficiency laser diodes based on QWs and QDs emitting at different wavelengths. The final goals of this activity are twofold: firstly to provide the fabrication partners with design recommendations and secondly, to gain, based upon the simulations, an understanding of the

underlying physics that determines the behaviour of the devices, which can then help in the design optimisation.

UPM is extending a previous simulation model and code for high power and high brightness laser diodes in order to include active layers based on Quantum Dots and to consider satellite valleys in the Conduction Band, for a proper simulation of red-emitting devices.

Based on the simulation results, properly validated by comparison with experiments, UPM is providing the fabricating partners with design recommendations for red-emitting Broad Area (BA) lasers, 975 nm and 1060 nm high-brightness tapered lasers based on QWs, high wall-plug efficiency 975 nm BA lasers, and 920 nm and 1060 nm QD-based tapered lasers.

UPM is also contributing to a better understanding of the facet heating and Catastrophic Optical Damage (COD) limitations in red lasers by simulating the facet heating in comparison with the experimental results provided by MBI. Design recommendations will be made on how to improve the reliability of high power red lasers.



*Simulation of the normalised forward (top) and backward (bottom) field intensity profile of an index guided tapered laser.*

### Further Information

Further information can be obtained from:

Professor Ignacio Esquivias

Tel: +34 913 367 339

E-mail: [esquivia@tfo.upm.es](mailto:esquivia@tfo.upm.es)

Web: <http://www.tfo.upm.es>

## Ferdinand Braun Institute

The Ferdinand-Braun-Institut für Höchstfrequenztechnik (FBH) explores cutting-edge technologies in the fields of microwaves and optoelectronics. It develops high-frequency devices and circuits for applications in communications and sensor technology. High-power diode lasers with excellent beam quality are the major optoelectronics research topic. Applications of such devices include materials processing, laser technology, medical technology and high precision metrology.

FBH's diode lasers are highly requested for solid-state laser pumping, optical communications, direct materials processing and laser displays. The institute also carries out basic investigations on nitrides for applications such as UV light sources or transistors for very high voltages.

It develops customised semiconductor lasers and circuits for research and industry. The activities cover all device steps ranging from epitaxial layer design and growth, processing and characterisation to reliability tests.

In the field of high-power diode lasers, FBH's activities focus on the R&D of novel laser diodes and systems. Covering the whole value chain, FBH investigates different types laser diodes from the visible to near infrared. The main objectives are further enhancement of brightness and beam quality, increasing efficiency and improvement of reliability of high-power laser diodes. Other activities also include fundamentally new approaches in design as well as continuous improvement of materials, based on the institute's profound know-how in manufacturing tailor-made diode lasers.



FBH's R&D in microwaves and optoelectronics are based on the same fundamental technologies. As an internationally recognised centre of competence for III-V compound semiconductors, FBH operates industry-compatible and flexible clean room laboratories with vapour phase epitaxy and a III-V semiconductor process line. Work is based on comprehensive materials & process analysis equipment, a state-of-the-art device measurement environment and excellent tools for simulation and CAD. In close cooperation with industry, its research results lead to cutting-edge prototypes.

## Activities within WWW.BRIGHTER.EU

In BRIGHTER, FBH is developing new diode lasers for three applications and devices have been delivered to project partners for implementation into new systems.



### LASER DISPLAY APPLICATIONS

*Nearly diffraction-limited red laser sources* - The target is a maximum output power of 1W and a reliable output power of 500mW. The tapered devices have separate contacts for the RW & tapered sections allowing high-frequency modulation with small RW currents. After two years, a maximum output power of ~700mW together with an excellent beam quality was obtained.

*1060nm DBR tapered lasers for green light sources based on second harmonic generation* - A maximum output power of 12W was obtained with a diffraction-limited beam quality and narrow spectral linewidth. These lasers can be modulated at frequencies up to 1GHz and show reliable operation at 5W over >1000h.

### MEDICAL APPLICATIONS

*650 nm BA lasers & bars for photodynamic therapy* - Devices with a record high reliability were developed. 100µm stripe lasers worked at a power of 1W for more than 10,000h. 5mm wide bars consisting of ten 100µm wide emitters also achieve a lifetime of >10,000h at 7W.

*670nm & 810nm tapered gain media for extended cavity laser systems* - The ECL systems will be used as pump sources for frequency conversion into blue and UV. At 670nm, the devices are capable of a maximum peak power of ~3W, the 810nm tapered gain media of ~27W.

*670nm tapered lasers for a fluorescence molecular imaging system* - A maximum cw output of 1W was obtained with a nearly diffraction-limited beam quality.

### TELECOM APPLICATIONS

*1060nm DBR tapered laser for optical wireless comms.* - Twin contact high-brightness devices were developed and are suitable for efficient Gbit/s transmission.

### Further Information

Priv.-Doz. Dr. Bernd Sumpf

Tel: +49 30 6392 2659, Fax: +49 30 6392 2642

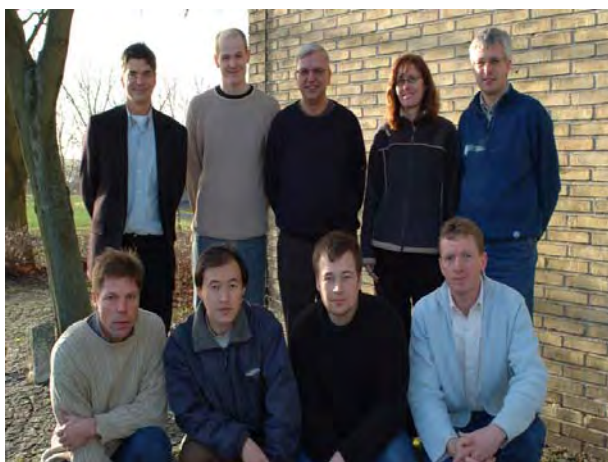
Email: bernd.sumpf@fbh-berlin.de

Web: [www.fbh-berlin.com/business-areas/diode-lasers](http://www.fbh-berlin.com/business-areas/diode-lasers)

## DTU Fotonik

The diode laser research team that is responsible for developing novel external feedback lasers within the BRIGHTER project is part of DTU Fotonik at the Technical University of Denmark. This research group carries out fundamental studies as well as applied research. New diode laser systems for medical applications, materials processing, biotechnology and optical sensing are developed. An important research area for the team is the development of new high-power, tunable diode lasers with high spatial and temporal coherence and the application of these new laser systems in second harmonic generation.

Nonlinear optics has been a research subject of intense investigation for many years in the group. The field covering the dynamics of optical materials is concentrated on inorganic materials. The efforts here have been within photorefractives and semiconductors in which nonlinear effects such as parametric oscillation and amplification, optical phase conjugation and four-wave mixing have been studied.



*The diode laser group outside the lab in Denmark.*

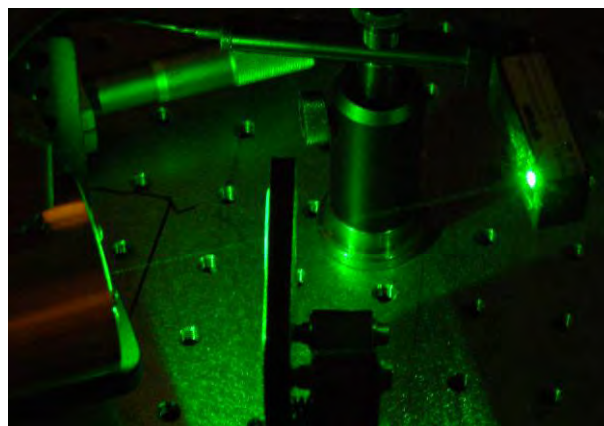
### Activities within WWW.BRIGHTER.EU

DTU Fotonik coordinates the activities within the work package “External cavity approaches to high brightness and tunability”, where the goal is to improve the spectral characteristics and beam quality of high-power diode lasers to yield nearly diffraction-limited tunable lasers.

As part of the research and development carried out, DTU Fotonik develops new external laser architectures that significantly improve the temporal coherence properties, wavelength selectivity, wavelength tuning range, and brightness of high-power broad-area diode lasers, tapered lasers and laser bars.

One recent example is the successful application of tapered amplifiers with external feedback providing virtually single frequency operation of diode lasers with several Watts of output power. These laser systems have been successfully frequency-doubled into the blue wavelength region (400nm).

In WWW.BRIGHTER.EU, the group at DTU Fotonik also participate in the activities *Medical Laser Systems* and *Laser Sources for Display Applications*. Within *Medical Laser Systems*, one important goal for DTU Fotonik is to develop blue lasers for fluorescence diagnostics of various cancer types. While DTU Fotonik is producing prototype systems for clinical testing, other partners in the Consortium are responsible for carrying out clinical trials using them. Within *Laser Sources for Display Applications*, DTU Fotonik develops and evaluates high-brightness green SHG laser sources with 100MHz modulation.



*Within the BRIGHTER project DTU Fotonik is developing green laser sources based on single pass SHG. More than 450mW of green light at 531nm has been obtained to date.*

### Further Information

Further information can be obtained from:  
 Paul Michael Petersen, Head of Research  
 Tel: +45 4677 4512  
 E-mail: paul.michael.petersen@risoe.dk  
 Web: <http://www.dtu.dk>

### *In the next e-Newsletter...*

Look out for profiles of Biolitec AG, Thales Research and Technology, Tyndall National Institute and the Institute of High Pressure Physics, UNIPRESS, in the next e-Newsletter coming in March 2009. If you want to find out more about these partners now, or indeed any of the other partners in the project, please visit our website at <http://www.ist-brighter.eu>.

## Recent Progress in Interstitial Photodynamic Therapy for Solid Tumors

Dr. Susanna Gräfe

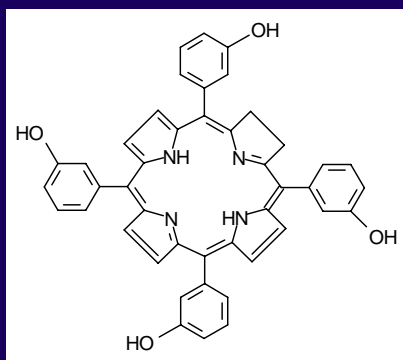
biolitec AG, Jena, GERMANY

Photodynamic therapy, PDT, has a nearly one hundred-year history. However, it is still a relatively new therapy option for the treatment of malignancies using light and a suitable photosensitizer (Rodriguez *et al.*, 2004). The term “photodynamic action” was first described and defined by Hermann von Tappenheimer in Munich in 1904. However, it would take another 60 years until Lipson and Baldes reported that neoplastic tissues containing a photosensitizer could fluoresce when excited by UV light (Huang, 2005). PDT was rediscovered and brought to a worldwide audience in the late 1970s by Thomas Dougherty (Allison *et al.*, 2006).

### Photosensitizers for PDT

After this rediscovery, a whole flood of new photosensitizers were reported in the 1980s and 1990s, most of which belong to the porphyrin family. The first commercially available photosensitizer, Photofrin, was approved for PDT of cancer of the lung and the esophagus (Dougherty *et al.*, 1998). Photofrin is a complex mixture of hematoporphyrins, HpD (Lipson *et al.*, 1961). In addition, the use of Photofrin is limited by its weak absorption of red light that penetrates the tissue and also its tendency to accumulate in healthy tissue, like the skin and thus cause a photosensitization of the skin. During the last 20 years, only a few other photosensitizers have been officially approved for PDT of a diverse range of malignancies. One of these is Temoporfin (Foscan®, meta tetrahydroxyphenylchlorin, m-THPC, biolitec AG), a photosensitizer belonging to the second generation of photosensitizers. Temoporfin is activated with non-thermal light at a wavelength of 652 nm delivered by a laser 4 days after intravenous administration of the drug.

### Temoporfin



Molecular Formula:  $C_{44}H_{32}N_4O_4$

Molecular Weight: 680.24

7,8-dihydro-5,10,15,20-tetrakis-(3-hydroxyphenyl) porphyrin.

Soluble in Alcohol and practically insoluble in all aqueous media

Figure 1: Characteristics of Temoporfin (Foscan®), a second generation photosensitizer.

## A PDT Treatment Regime

Foscan®-mediated PDT is a loco-regional therapy for the palliative treatment of patients with advanced head and neck squamous cell carcinoma who have failed prior therapies and are unsuitable for radiotherapy, surgery or systemic chemotherapy. PDT with Foscan® represents a significant therapeutic advance in the treatment of head and neck cancer. The recommended drug dose is 0.15 mg/kg, followed 96 hours after drug administration with a laser light dose of 20 J/cm<sup>2</sup>, delivered at 100 mW/cm<sup>2</sup> (Foscan® Product Monograph, biolitec pharma Ltd.).

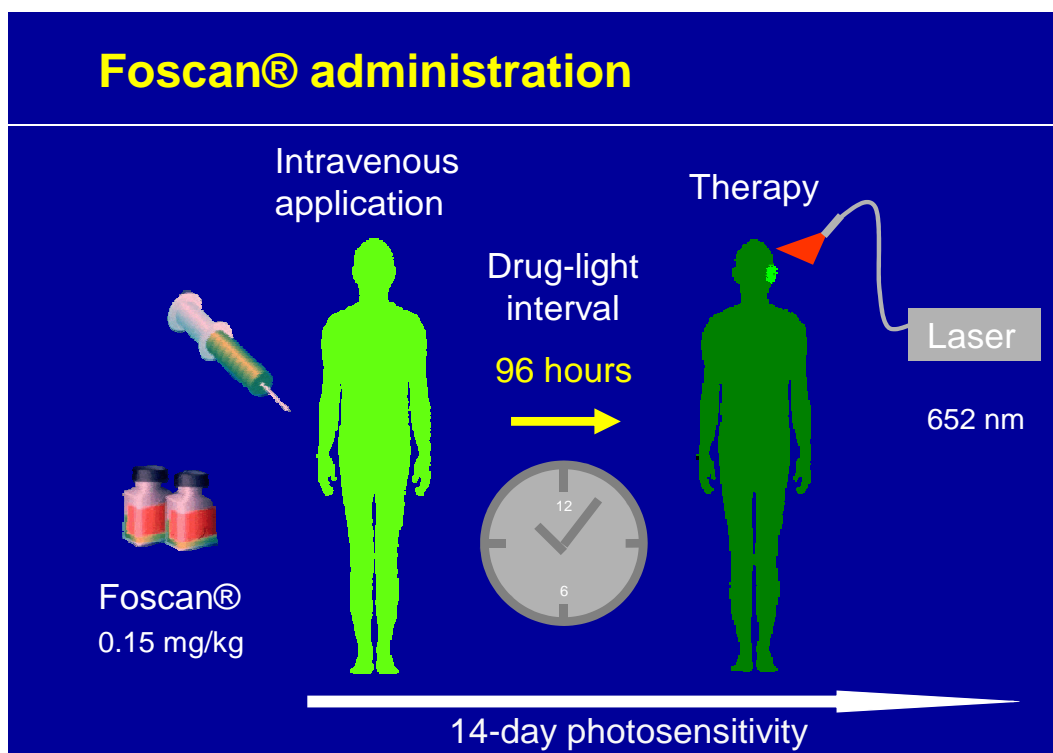


**Figure 2: Scheme of PDT using Foscan®.** After intravenous Foscan® administration and a drug-light interval (DLI) of 96 hours, the tumor tissue is illuminated by 652 nm laser light.

## PDT Treatment Mechanism

Since the PDT contains a photosensitizing mechanism, three main variables are enclosed into the effective process: localization of the photosensitizer, its pharmacokinetics and its photophysics. For the actual treatment, three ingredients are required: the photosensitizer, a light source, usually a laser, suitable to activate the photosensitizers' photophysics and a method of applying the right dose of light in the target location.

An efficient photosensitizer should therefore be phototoxic, but not toxic. This requires a selective retention of the substance in the tumor tissue and a greater photosensitizer clearance of normal tissue in comparison to tumor tissue. For their activation, photosensitizers need light of a suitable wavelength belonging to the absorption spectra of the photoactive substance. The photosensitizer absorption is of crucial importance, since the light penetration into the tissue is improved with a rising wavelength of the light (Bourré *et al.*, 2002).

A substance, which is a photosensitizer, is enriched in tumor tissue and illuminated with light of a defined wavelength. The coincidence of light with the photosensitizer in the tissue leads to the formation of singlet oxygen, which acts as a cellular poison and can destroy the exposed cells.

## PDT Chemistry

Usually the photosensitizer is activated from a ground singlet state to an excited singlet state by light of a specific wavelength. Subsequently, it undergoes intersystem crossing to a longer-lived excited triplet state. There are only few chemical species in the tissue with a ground triplet state. One of them is molecular oxygen. When the photosensitizer and an oxygen molecule come close together, an energy transfer can take place. The energy transfer allows the photosensitizer to relax to its ground singlet state and thus to repeat the same process creating further excited singlet state oxygen molecules. The singlet state oxygen molecules interact very rapidly with any biomolecule in the surrounding region and it is this destructive reaction which kills cells through apoptosis or necrosis (Wikipedia, Photodynamic therapy). Due to the very short half-life of  $^1\text{O}_2$ , this cytotoxic molecule can only diffuse 20 nm in cells (Moan *et al.*, 1991).

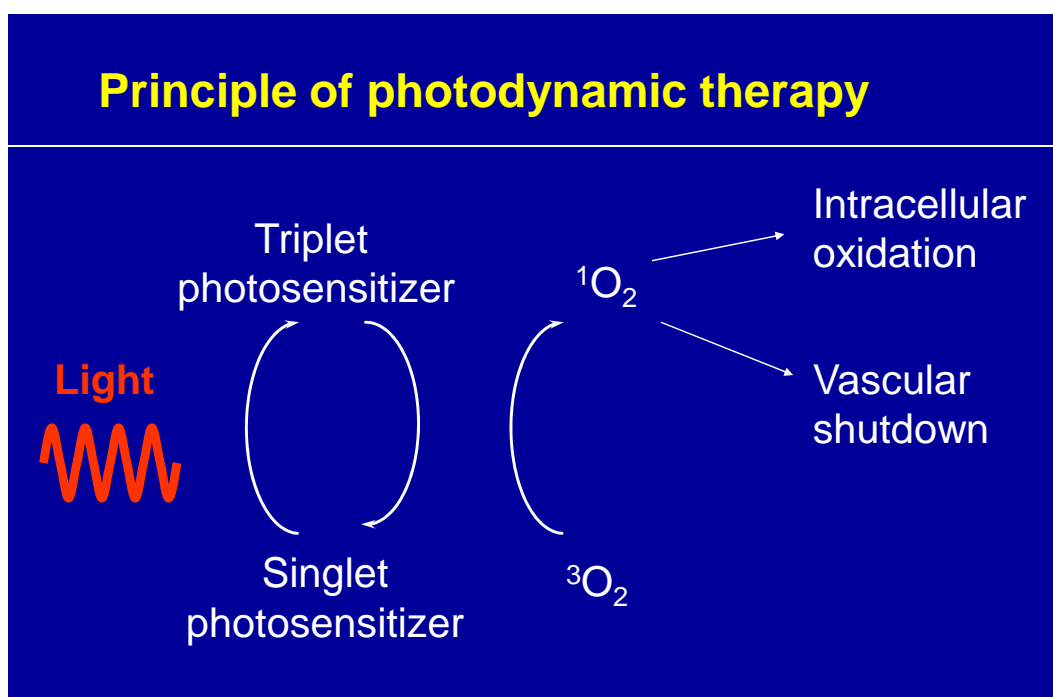


*Figure 3: Principle of PDT – formation of a singlet oxygen by interaction of molecular oxygen in the tissue with a photosensitizer molecule excited to its triplet state by light of a specific wavelength.*

## Lasers for PDT

Whilst the very first treatments were conducted with bulky and maintenance intensive lasers, like Argon-ion pumped dye lasers, the first diode laser based systems became available in the middle of the 1990s. These devices were already lightweight, easy-to-handle, air-cooled systems, and thus allowed a major step forward in spreading PDT as a viable treatment option. European projects like Ultrabright, developing 730-760nm laser diodes, WWW.BRIGHT.EU and most recently WWW.BRIGHTER.EU, developing 630-680nm diode lasers have led and continue to lead to highly reliable, high-power, cost-efficient laser sources, which will eventually enable the development of PDT for a much larger variety of indications. Consequently, PDT has developed into a most promising therapy for malignant tumors during the last few years. A principal purpose of the PDT in tumor treatment should always be the selective destruction of malignant cells, without damaging healthy tissue and to maintain its complete functionality. Unfortunately, it is often difficult to realise this aim.

## Medical Use of PDT

Medical applications of PDT have been developed especially for the skin, e.g. the treatment of psoriasis (Zanolli, 2004; Cather & Menter, 2002) or basal cell carcinoma (Bendsoe *et al.*, 2007). With the increasing technical progress in the development of both lasers and light conductor technology, it has become possible to also deliver light to internal organs, thus increasing the medical interest of PDT. However, PDT has mainly been used to treat superficial malignant or premalignant skin lesions or mucosa lesions, which are easily reachable by bare fibres or via an endoscope (Vogl *et al.*, 2004). Due to the limited tissue penetration of the light and the necessity to activate the photosensitizer locally, the therapeutic options have so far been restricted.

## Interstitial PDT

During the last few years, interstitial PDT (IPDT) was developed and is being used more and more to deliver light into tissues and organs deep under the skin via fibres. Specially developed diffuser fibres guarantee a sufficient light distribution for PDT. Another advantage of interstitial PDT is the lack of tumor size restriction. Interstitial PDT can be used for a wide range of applications.

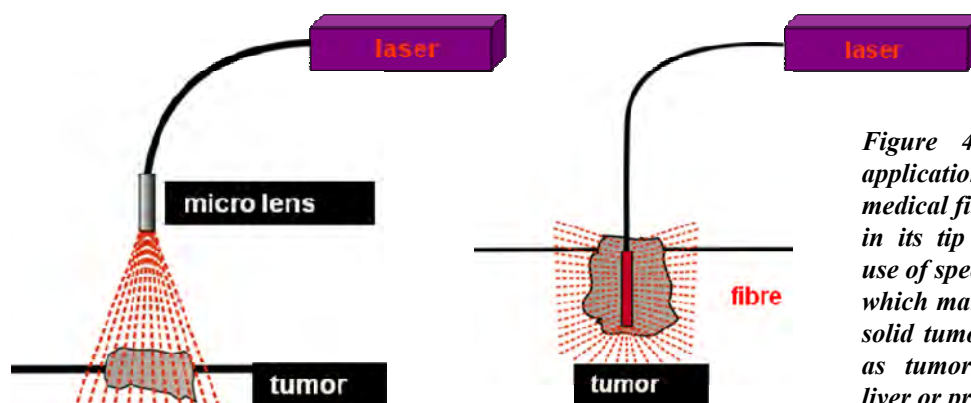


*Figure 4: Superficial light application on the skin using a medical fibre with a micro lens in its tip (left) and IPDT by use of special light applicators, which make it possible to treat solid tumors in the body such as tumors of the pancreas, liver or prostate (right).*

## Recent Progress in Interstitial PDT

In 2001, Tanaka and co-workers published their work about interstitial PDT of patients with squamous cell carcinoma of the tongue. Three patients were treated by the use of Photofrin as the photosensitizing agent. A complete response without any complications and functional disabilities was reached in two patients. One patient showed only a partial response to this therapy.

Engelmann *et al.* (2003) demonstrated that PDT could be an effective and feasible therapy for the treatment of liver metastases. The study was part of a multicenter phase-I-study. Five patients suffering from colorectal liver metastases were treated by PDT. For the PDT, the photosensitizer SQN400 and interstitial photodynamic laser treatment were applied. The PDT effect was monitored by contrast-enhanced computer tomography (CT) 1 cm around every single fibre. A complete necrosis within a radius of 1 cm was detectable.

Another study, by Betz and co-workers (2007), described the interstitial PDT of 11 patients with lymphatic or venous malformation by the use of Foscan®. Four days after intravenous administration of 0.15 mg/kg of Foscan® the tissue to be treated was illuminated by 652 nm light and bare tip fibres at a total light dose of 20 J per fibre. The PDT result was evaluated by MRI-imaging, CT-volumetry and surface optical scanning. A significant reduction of abnormal tissue without damage of healthy skin was detectable in all treated patients, especially for lymphatic malformations, where the best results were obtained.

IPDT has also developed as an alternative for radical prostatectomy and radiation therapy (Moore *et al.*, 2005). Temoporfin was used for the IPDT of secondary and primary prostate cancer. IPDT resulted in a significant necrosis of the prostate tissue and the prostate-specific antigen (PSA) was decreased.

Another study about IPDT of recurrent prostate cancer was published by Weersink *et al.* (2005). The vascular-targeted photosensitizer TOOKAD was used in these studies. These studies demonstrated that IPDT can present a relatively safe alternative treatment for prostate cancer.

A lot of other IPDT studies have been published and demonstrate a common problem of this therapy option: the ideal light dose for the treatment is generally unknown and therefore an investigation about the dosimetry of the light is strongly recommended. There are large intra- and inter-patient variations due to the biological variations of the tissue and the individual response to the therapy. Johansson *et al.* (2007) therefore developed a real-time dosimetry software tool for IPDT of the human prostate and have investigated algorithms that can analyse the light distribution within the target tissue.

The future prospects of IPDT are very promising. The further development of light sources, light applicators for IPDT and new target-orientated photosensitizers will make an exact dosimetry feasible and reduce the possible adverse effects to a minimum. It is likely that IPDT could become the first choice of therapy for different malignancies within the next few years.

## References

- Allison R., Bagnato V.S., Cuenca R., Downie G.H. & Sibata C.H., *The future of photodynamic therapy in oncology*. Future Oncol. 2(1):53-71 (2006)
- Bendsoe N., Persson L., Johansson A., Axelsson J., Svensson J., Gräfe S., Trebst T., Andersson-Engels S., Svanberg S. & Svanberg K., *Fluorescence monitoring of a topically applied liposomal formulation and photodynamic therapy of non-pigmented skin malignancies*. JEPTO, 26(2):117-126 (2007)
- Betz C.S., Jäger H.R., Brookes J.A.S., Richards R., Leunig A. & Hopper C., *Interstitial photodynamic therapy for a symptom-targeted treatment of complex vascular malformations in the head and neck region*. Lasers in Surgery & Medicine 39:571-582 (2007)
- Bourré, Rousset, Thibaut, Eleouet, Lajat & Patrice, *PDT effects of m-THPC & ALA, phototoxicity & apoptosis*. Apoptosis, 7:221-230 (2002)
- Cather J. & Menter A., *Novel therapies for psoriasis*. Am J. Clin. Dermatol. 3(3):159-173 (2002)
- Dougherty, Gomer, Henderson, Jori, Kessel, Korbelik, Moan & Peng, *Photodynamic Therapy: Review*. J. Nat. Cancer Inst. 90:889-902 (1998)
- Engelmann K., Mack M.G., Eichler K., Straub R., Zangos S. & Vogl T.J., *Interstitielle photodynamische Lasertherapie zur Behandlung von Lebermetastasen: Erste Ergebnisse einer in vivo Phase I-Studie*. Röfo Fortschr Geb Röntgenstr Neuen Bilgeb Verfahr 175:682-687 (2003)
- Foscan® Product Monograph, biolitec pharma Ltd.
- Huang Z., *A review of progress in clinical photodynamic therapy*. Technol. Cancer Res. Treat. 4(3): 283-293 (2005)
- Johansson A., Axelsson J & Andersson-Engels S., *Realtime light dosimetry software tools for interstitial photodynamic therapy of the human prostate*. Med. Phys. 34(11):4309-4321 (2007)
- Lipson, Baldes & Olsen, *The use of a derivative of hematoporphyrin in tumor detection*, JNCI, 26:1 (1961)
- Moan J. & Berg K., *The photodegradation of porphyrins in cells can be used to estimate the lifetime of singlet oxygen*. Photochem. Photobiol. 53:549-553 (1991)
- Moore C., Hoh I., Bown S & Emberton M., *Does photodynamic therapy have the necessary attributes to become a future treatment for organ-confined prostate cancer?* BJU Int. 96(6):754-758 (2005)
- Rodriguez E., Baas P., Friedberg J.S., *Innovative therapies: photodynamic therapy*. Thorac. Surg. Clin. 14(4):557-66 (2004)
- Tanaka H., Hashimoto K., Yamada I., Masumoto K., Ohsawa T., Murai M. & Hirano T., *Interstitial photodynamic therapy with rotating and reciprocating optical fibers*. Cancer 91(9):1791-1796 (2001)
- Vogl T.J., Eichler K., Mack M.G., Zangos S., Herzog C., Thalhammer A. & Engelmann K., *Interstitial photodynamic therapy in interventional oncology*. Eur. Radiol. 14:1063-1073 (2004)
- Weersink R., Bogaards A., Gertner M., Davidson S., Zhang K., Netchev G., Trachtenberg J. & Wilson B., *Techniques for delivery and monitoring of TOOKAD (WST09-)mediated photodynamic therapy of the prostate: Clinical experience and practicalities*. J. Photochem. Photobiol. B79(3):211-222 (2005)
- Wikipedia, *Photodynamic Therapy*. Accessed online [www.wikipedia.org](http://www.wikipedia.org), October 2008
- Zanolli M., *Phototherapy arsenal in the treatment of psoriasis*. Dermatol. Clin. 22(4):397-406, (2004)

## External Cavity Lasers:

### Recent Developments within BRIGHTER

Zhichao Zhang, Lei Lang, Jun Lim, Stephen Bull, Slawomir Sujecki, Eric Larkins  
The University of Nottingham, University Park, Nottingham, NG7 2RD, U.K.

David Paboeuf, Gaëlle Lucas-Leclin, Nicolas Dubreuil, Gilles Pauliat, Patrick Georges  
Laboratoire Charles Fabry de l'Institut d'Optique, CNRS, Univ Paris-Sud, RD128, 91127 Palaiseau, FRANCE

Mingjun Chi, Jesper Holm, Ole Bjarlin Jensen, Birgitte Thestrup, Peter E. Andersen, Paul Michael Petersen  
DTU Fotonik, Technical University of Denmark, Frederiksborgvej 399, 4000 Roskilde, DENMARK

Christian Larat

Thales Research & Technology France, Avenue de la Vauve (RD128), F-91767 Palaiseau Cedex, FRANCE

Karl-Heinz Hasler, Bernd Sumpf, Hans Wenzel, Götz Erbert

Ferdinand-Braun-Institut für Höchstfrequenztechnik, Gustav-Kirchhoff-Straße 4, D-12489 Berlin, GERMANY

Nicholas Michel, Myriam Oudart, Michel Krakowski

Alcatel-Thales III-V Lab, Route de Nozay, F-91461 Marcoussis Cedex, FRANCE

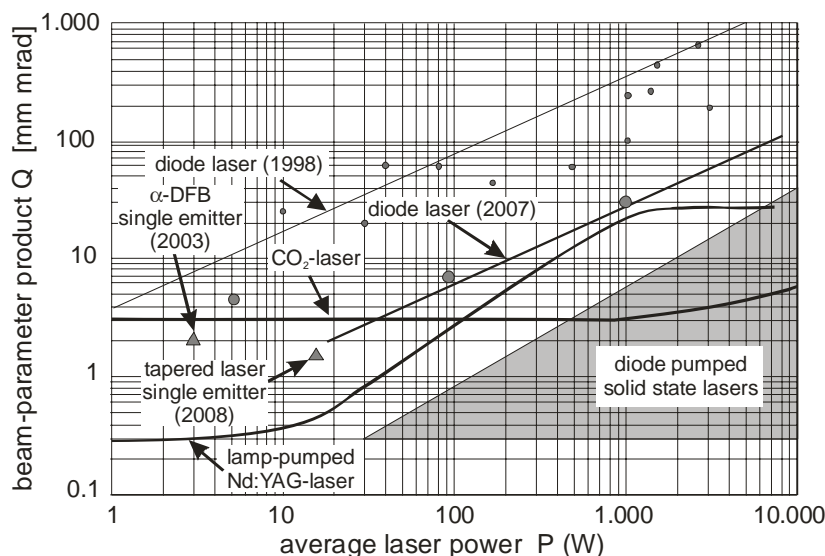
Peter Loosen

Fraunhofer Institute for Laser Technology, Steinbachstraße 15, D-52074 Aachen, GERMANY

High-brightness semiconductor lasers have been the key components for the success of many technologies. A good example is optical telecommunications where the introduction of laser diode pumps made erbium glass based technology a viable solution for signal amplification in optical fibre links. Other successful applications of high-power semiconductor laser diodes are in medicine, pollution monitoring, display technology, printing and manufacturing.

The compactness, cost, simple pumping mechanism and reliability of semiconductor laser diodes are their main advantages. The three laser diode structures, which are used to produce beams with high output power are the broad-area laser, the tapered laser and the laser bar. The key parameter of the usability of these laser diode sources is their brightness. The higher the brightness, the higher the power delivered in a small spot. Brightness is the optical power per emission area and unit of solid angle of the output beam and can be expressed as:

$$B = \frac{P}{A\Omega} \propto \frac{P}{Q^2} = \frac{P}{(\omega_0\Theta_f)^2} \propto \frac{P}{(M^2)^2}$$



The brightness is related to  $M^2$  and the *beam parameter product*  $Q$  (product of the minimum diameter  $\omega_0$  & the divergence  $\Theta_f$  of the beam). Figure 1 describes the state-of-the-art for the power and the brightness of high-power diode lasers and systems.

**Figure 1: State-of-the-art for the brightness of laser diodes and systems.**

To achieve a higher brightness, we can either increase the available power or increase the beam quality by reducing the beam parameter product. Given a specific optical source, neither of these two means for brightness improvement can be achieved using passive components like lenses, mirrors, pinholes, etc. In fact, due to its imperfections, an optical system can only decrease the brightness of a beam. However, it is possible to increase the available brightness of a laser diode or bar by operating it in an external cavity. A number of external cavity concepts have been developed for this purpose. These concepts rely upon one of several approaches, including: a) the use of external feedback to force the laser to oscillate in a single or small number of modes; b) wavelength multiplexing to spatially overlap and combine multiple beams; and c) phase-locking to force multiple emitters to lase in the same optical mode. For example, the brightness and spectral brightness of single emitter laser diodes can be improved by using external cavities with appropriately designed feedback mirrors and/or gratings. The brightness of laser diode bars can be improved to achieve very high power levels with good beam quality using various beam multiplexing schemes or phase coupling methods.

Often, we are interested not only in the brightness of a laser beam, but also its *spectral brightness*, which can be defined as its brightness divided by its spectral width (measured at the  $1/e^2$  points):

$$SB = B/\Delta\lambda$$

High spectral brightness is of particular interest for frequency doubling, as the wavelength conversion efficiency increases superlinearly with power. Thus, in addition to improving brightness, the external cavity schemes are also used to widen the area of application of laser diode sources by using frequency doubling to reach shorter wavelengths. Here, the external cavity is used to improve *both* the brightness and the spectral brightness of the source being doubled.

In this article, we report on the work performed within the WWW.BRIGHTER.EU project on the development of external cavity lasers for applications in medicine, display technology and telecoms. This work includes both the practical realisation of the lasers as well as extensive work on their modelling and design. The particular external cavity lasers discussed in this paper include: self-organised external cavity laser diodes, laser diodes with asymmetric feedback, frequency doubling, laser bar beam combining and phase-locking with an external Talbot cavity. We also give a brief description of the developed modelling and design tools together with example simulation results.

### **Self-organised extended cavities with tapered amplifiers**

A well-established procedure to reduce the linewidth of a tapered laser is to insert the tapered device inside an extended cavity containing a spectral filter, such as a diffraction grating. Although this technique is quite efficient, it presents the disadvantage of requiring adjustments: the maximum reflectivity of the diffraction grating has to be adjusted to the mode selected by the operator [1]. Because the exact mode position depends on the cavity length, the cavity may have to be re-adjusted if the cavity parameters change, typically following ageing or just following a change of the thermal load.

To overcome this inconvenience, we previously proposed the concept of self-organised extended cavities. Applied to a tapered device, a self-organised cavity is quite similar to a conventional extended cavity containing the tapered amplifier. Instead of a fixed selective element, a dynamic holographic recording medium (photorefractive crystal) is inserted in the cavity. We have previously shown that the continuous adaptation of the oscillating modes with the dynamic hologram they record forces the laser source to oscillate on a single longitudinal mode without modifying the spatial quality of the beam. The self-adapting process preserves the single mode oscillation by adapting the dynamic hologram even if the cavity parameters, (temperature, electrical pumping, etc.) change. This process is fully transparent to the user, as it requires no intervention.

Photographs of one of the self-organised extended cavities developed by LCFIO are shown in Fig. 2. Typically, these cavities provide optical beams with powers larger than 1 W and coherence lengths larger than a few meters without any mode hopping over a period of one day. The side mode suppression ratio is larger than 30 dB with a  $M^2$  parameter lower than 2. The cavity adapts itself to any change. If the temperature or the current changes, the cavity adapts itself to insure single mode oscillation. The adaptation time is about 30 s. Typical spectra are shown in Fig. 3 for various currents. For any temperature or current, the cavity finds, by itself, the best filtering characteristics to achieve the highest output on a single mode without any adjustment by the user.

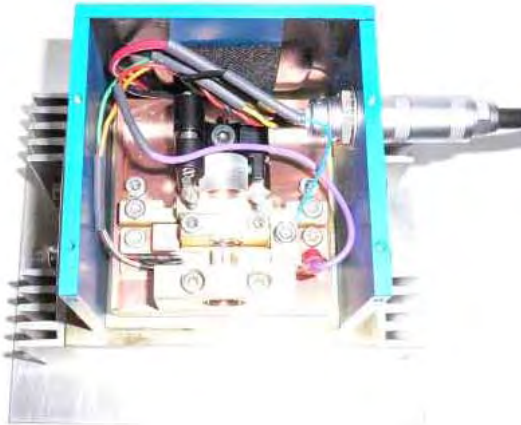


Figure 2: Photograph of one of the self-organised cavity lasers developed by LCFIO.

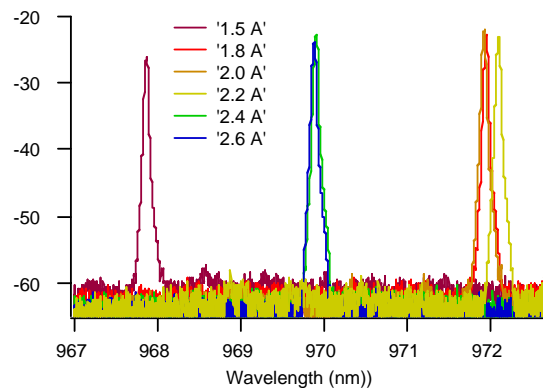


Figure 3: Typical single mode spectra obtained from a self-organised cavity laser for various currents.

### External cavity lasers with asymmetric feedback

In WWW.BRIGHTER.EU, DTU Fotonik develops new external feedback diode laser techniques that improve the coherence properties of high-power diode lasers to yield nearly diffraction-limited tunable single mode lasers. Moreover, this work focuses on the development of compact, low-cost blue and ultraviolet frequency doubled lasers. Here, we discuss frequency doubling in a new external cavity configuration with a pulsed output of up to 720 mW at 404 nm using an 808 nm tapered diode laser as the pump source. The laser system is used in WWW.BRIGHTER.EU for biomedical fluorescence diagnostics applications.

#### Single mode tunable 808 nm laser source

The 808 nm tapered diode amplifier used in our external cavity experiments is based on a super large optical cavity (SLOC) structure developed at the Ferdinand Braun Institute in Berlin, Germany. The external cavity configuration employed is depicted in Fig. 4. The grating is mounted in the Littrow configuration and oriented with the lines of the grating parallel to the active region of the amplifier. The laser cavity is formed between the diffraction grating and the output facet of the tapered amplifier [2].

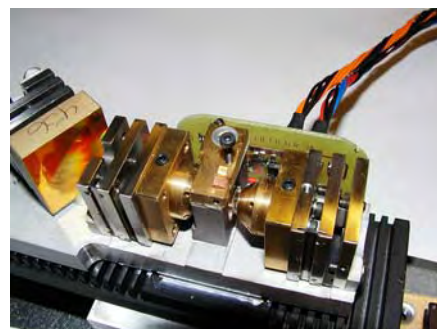
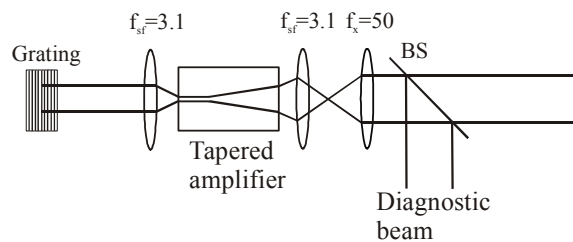


Figure 4: Experimental setup of the tapered diode laser system using a bulk diffraction grating external cavity with the units given in mm in the schematic (top) and the compact prototype of the laser source (bottom).

The output power at different wavelengths is shown in Fig. 5 for an operating current of 3.0 A. The laser system is tuned over a 29 nm range centred at 802 nm. The output power is above 800 mW over the 29 nm range. An output power as high as 1.95 W is obtained at 803.84 nm. In the range from 793 nm to 812 nm the output power is above 1.5 W.

The optical spectrum of the output beam from the tapered diode laser system is measured at the wavelengths of interest. Narrow linewidth (below 0.004 nm) operation is achieved over the 29 nm span. The sidemode suppression ratio is greater than 17 dB and the amplified spontaneous emission intensity is suppressed by more than 40 dB over the tunable range. The beam quality of the output beam along the slow axis is estimated by measuring the beam quality factor,  $M^2$ , for the external cavity laser system. The  $M^2$  value is below 1.3 over the 29 nm tunable range at a bias current of 3.0 A.

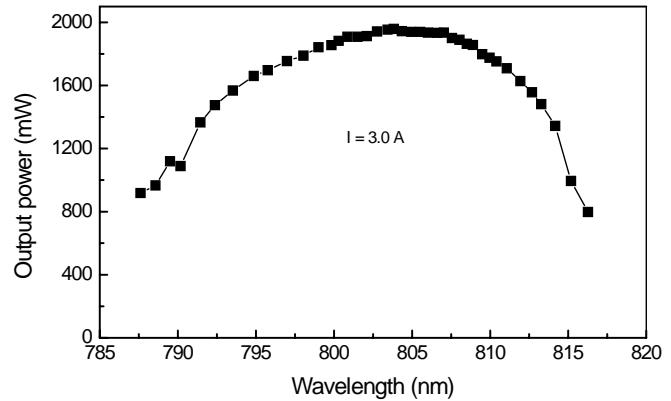


Figure 5: Tuning curve of the tapered diode laser system at an operating bias current of 3.0 A.

#### New blue laser system at 404 nm

In WWW.BRIGHTER.EU, DTU Fotonik has successfully implemented a 404 nm frequency-doubled laser module based on the tapered external feedback technology [3]. Using a very compact cavity design shown in Fig. 6, highly efficient frequency doubling has been demonstrated. The external cavity consists of two reflecting concave mirrors and a nonlinear crystal (ppKTP) placed between the mirrors. One of the mirrors in the cavity is controlled with a piezoelectric positioner and can be used to sweep the cavity in and out of resonance, which allows for pulsed (5  $\mu$ s to a few tens of microseconds) second harmonic generation. The piezoelectric mirror can either be externally controlled by a camera and a trigger system, or the mirror can be controlled through the use of an arbitrary waveform generator. This feature allows the system to be used in fluorescence imaging applications, where the blue laser pulses induce the fluorescence signal. Figure 7 shows the peak pulse power versus the coupled input power in the external cavity. The pulses produced have a peak power up to 720 mW. To the best of our knowledge, this is the highest SHG power obtained in ppKTP at 404 nm. In cw operation, an output power of 320 mW at 404 nm is obtained. The new SHG laser module has been used in WWW.BRIGHTER.EU for feasibility tests in biomedical fluorescence diagnostics applications.

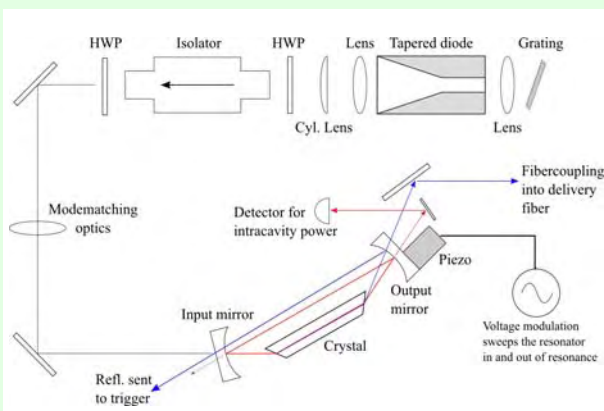


Figure 6: The experimental setup with SHG generation in an external cavity.

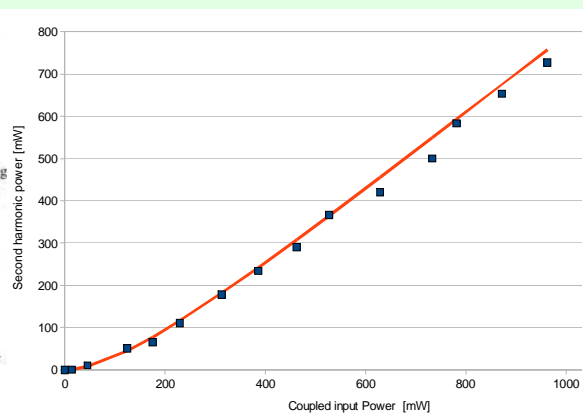
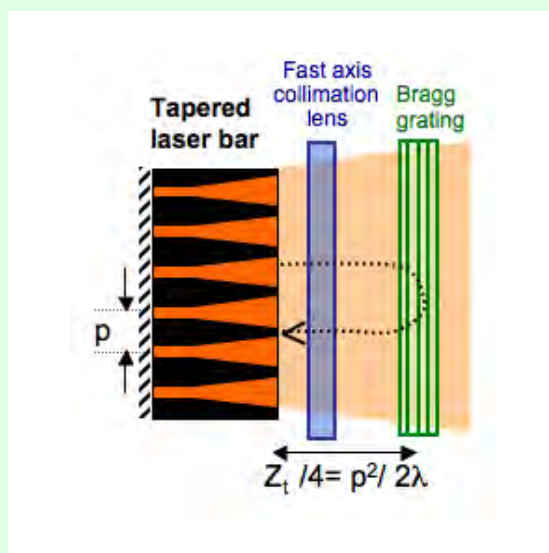


Figure 7: Experimentally measured blue peak power at 404 nm versus coupled pump power.

## Wavelength stabilisation and phase-locking of laser bars

A well-known way to enhance the beam quality of several lasers is to combine the beams coherently by inducing phase-locking of their beams. Within the framework of the WWW.BRIGHTER.EU project, the utilisation of the Talbot effect inside an external cavity is investigated by CNRS/LCFIO for that purpose. Furthermore, wavelength stabilisation of the whole bar to better than 0.2 nm is provided concurrently through the insertion of a spectrally selective component, which also acts as the external cavity mirror. The operation of this novel external cavity design, shown in Fig. 8, is explained below.

The Talbot effect describes the self-imaging properties of a periodic coherent field. It is a pure Fresnel diffraction phenomenon, which results from the free-space propagation of a periodic field. The source array produces an exact replica (in amplitude and phase) of the emitted field at integer multiples of the so-called Talbot distance  $Z_T$ , which is linked to the spatial period of the field. These self-imaging properties are applied to induce coherent coupling between the emitters of tapered laser bars in a specifically designed external cavity [4]. Actually, since the discrimination between the different spatial modes is a maximum for a propagation distance of  $Z_T/2$ , the external cavity length is chosen to be equal to  $Z_T/4$ . This enables the laser bar to operate in a single spatial supermode with all of the emitters in phase.



**Figure 8: External cavity setup for the phase-locking and coherent combining of a laser bar.**

Moreover, a volume Bragg grating (VBG) plays the role of the output coupler of the laser cavity and forces the laser emission of the entire bar to the same wavelength. Indeed, these gratings appear to have become essential optical components in recent years, with a high spectral selectivity ( $\sim 0.2$  nm), low loss, limited wavelength drift ( $\sim 0.01$  nm/°C) and a reflectivity from a few % to 100 % [5]. They are realised in photosensitive glasses, which allow writing of periodic structures under UV illumination in order to make filters with the desired properties. Many different experiments have been already reported with VBG, ranging from the brightness improvement of broad area laser diodes [6] to the wavelength stabilisation of single emitters and bars [7-9].

As an example, this design has been investigated using a bar of 10 index-guided tapered lasers emitting around 975 nm, with a pitch,  $p = 100$   $\mu\text{m}$ , developed by III-V Lab within the WWW.BRIGHTER.EU project.

The rear and front facet coatings are highly reflective and anti-reflective ( $R < 10^{-3}$ ), respectively. The VBG is 0.7 mm thick, with a maximum reflectivity of 40% at 976 nm and an angular acceptance of  $2^\circ$ . In a very simple and compact ( $L_{\text{ext}} = 5$  mm) external cavity, coherent operation of the bar has been observed in the in-phase mode with a strong degree of coherence across the whole operating range. Furthermore, each emitter is locked to the Bragg wavelength (See Fig. 9) and remains stable irrespective of the operating current. The spectral bandwidth of the emission is reduced to less than 300 pm. The output power reaches 1.7 W ( $I_{\text{op}} = 4$  A) and is limited mainly by the laser device itself. This leads to a significant increase in the brightness of the bar and compares well with the performance of an optimised bar of these very emitters.

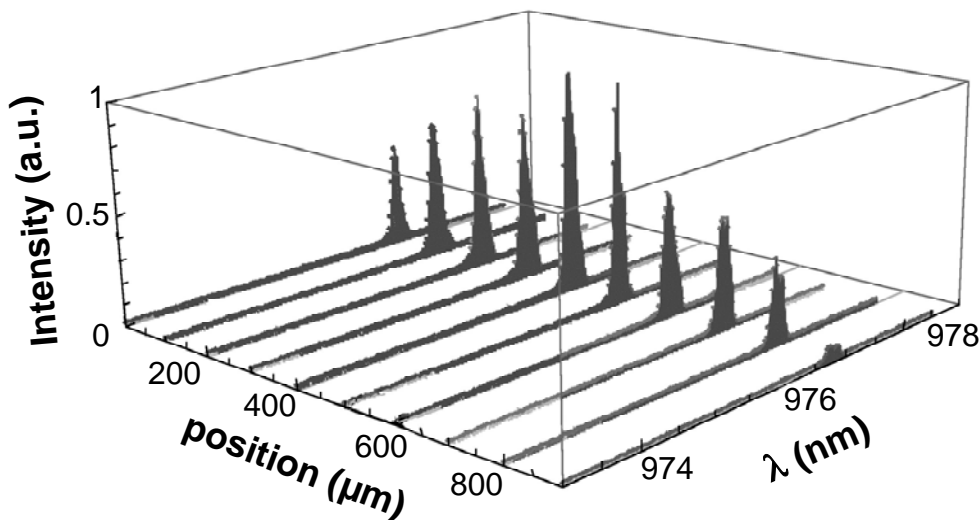


Figure 9: Spectrally resolved near-fields of the individual emitters in the external cavity.

These results are very promising for the realisation of compact high-power and high-brightness laser sources based on the tapered emitter bars developed within the framework of the BRIGHTER project by III-V Lab, FBH and ILT.

### Wavelength multiplexing of a laser diode bar

Less demanding systems, using incoherent sources, are possible only if the individual beams are perfectly superimposed spatially. In this case, the combined beam has (theoretically) the same beam quality as that of a single source. There are only two ways to do this:

- 1) the polarisation combination of two beams with orthogonal polarisation states  
(polarisation multiplexing)
- 2) the spectral combination of beams with different wavelengths  
(wavelength multiplexing)

The first solution is not really advantageous because it is limited to the combination of two beams, as a beam can exhibit only two polarisation states. On the other hand, wavelength multiplexing places no fundamental limit on the number of beams that can be combined (though there are practical limitations). We note that such a system, which uses passive optical components, does not infringe the earlier statement that the spatial brightness of a beam cannot be increased using a passive optical system. This is because the *spatial* brightness increase is paid back by a decrease in the *spectral* brightness (i.e. the combined beam spectral width is much larger than that of an individual beam).

A laser diode bar contains several incoherent laser diodes, which are regularly spaced in a plane. This makes the laser bar a very good candidate for a wavelength multiplexing experiment. We have used a bar with 30 tapered diodes developed within WWW.BRIGHTER.EU by Alcatel Thales III-V Lab. We have to force the diodes to emit at different wavelengths and then combine their beams with a spatially dispersive element. Actually, we use an external cavity using a grating to combine both the wavelength locking of the cavities and the wavelength multiplexing of their output beams. As seen in Fig. 10, after collimation of the fast axes, the beams of the emitters in the laser diode bar are collimated by a “Fourier lens.” This lens images the far-field from of each of the diodes in its image focal plane, where the grating is located. In this plane, all of the beams are superimposed (they have the same far-field), but with different angles of incidence. The output mirror is placed to reflect the first diffraction order of the grating. Thus, the cavity for each diode extends from the back side of the diodes (HR coated) up to the output mirror. Considering a single diode, the grating ensures that only a specific wavelength component of the beam reflected back from the output mirror is coupled back into the diode, forcing it to oscillate at this frequency. As each diode beam exhibits a different angle of incidence on the grating, the imposed wavelength is different for each diode. Finally, as the output mirror is flat, all of the beams are parallel after the grating. Thus, all of the beams are spatially superimposed, as desired.

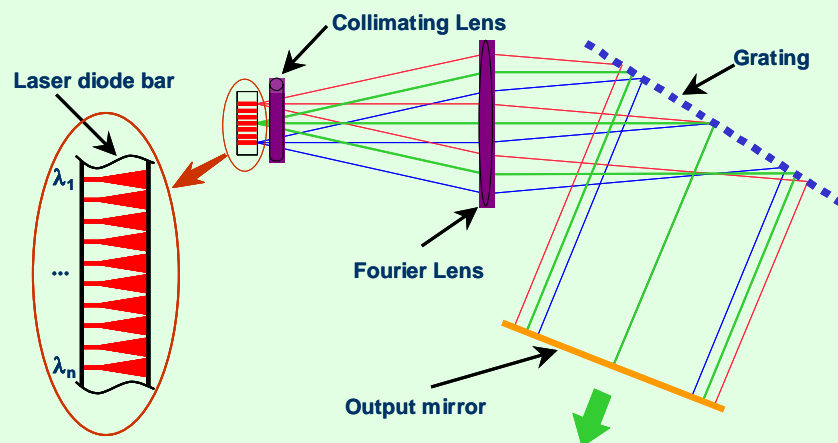


Figure 10: Cavity setup for the wavelength multiplexing of a laser diode bar

Figure 11 presents the spectral image of such a wavelength multiplexed laser diode bar. The output facet of the bar is imaged onto the entrance slit of a spectrometer via the zero order losses of the grating (not represented). Using a CCD camera in the output plane of the spectrometer, we can directly monitor the actual spectrum of each diode. In Fig. 11, the spectrum ( $\sim 15$  nm width) is horizontal and the lateral position within the bar ( $\sim 3$  mm width) is vertical. As expected, each diode exhibits a specific wavelength, leading to a linear repartition. In this case, the output power was 9 W for an injection current of 20 A.

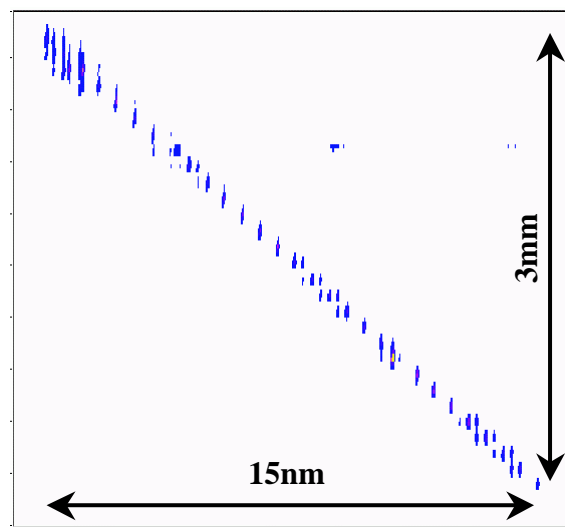


Figure 11: Resulting spectral image of a wavelength multiplexed laser diode bar.

## External cavity laser design and simulation

In order to achieve the optimal performance, external cavity lasers need to be designed using predictive design tools. Figure 12 shows a generic algorithm for an external cavity laser design tool. Such tools must include both an advanced semiconductor laser model and a good external optics model.

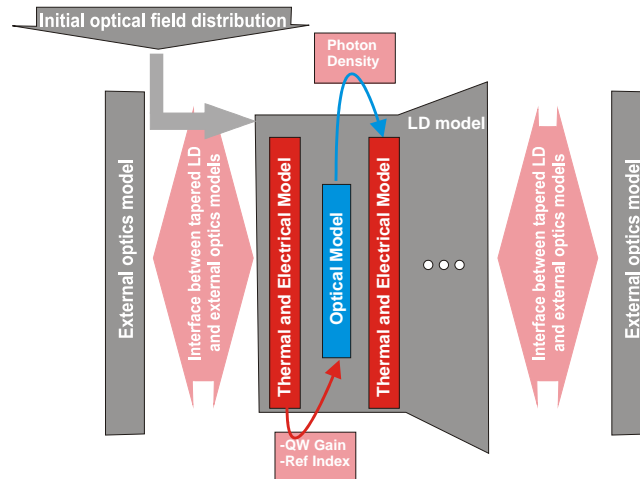


Figure 12: Flow chart of an external cavity laser model.

One example of an external cavity laser model developed within BRIGHTER is that used for a self-organising external cavity laser [10]. In this case, the laser diode model used is a multi-wavelength model [11]. The external cavity is treated as a self adapting Fabry-Perot filter [12], which provides a wavelength dependent feedback to the tapered amplifier. The semiconductor gain is calculated using a look-up table extracted from non-equilibrium gain simulations [13]. The calculated output spectrum of a tapered laser diode with a photorefractive crystal placed at the rear facet is shown in Fig. 13 (left). The spectrum when the PR crystal is not present is also shown for comparison. Figure 13 (right) shows the far-field pattern corresponding to the case where the PR crystal is used. The results indicate that at steady state, a single longitudinal mode is supported by the cavity. Without the PR crystal grating, the side modes have a round-trip gain comparable to that of the main mode, so that the cavity supports a broad longitudinal mode spectrum with a FWHM spectral width of more than 0.5 nm. The calculated far-field profile is approximately Gaussian with a FWHM of 2.5°.

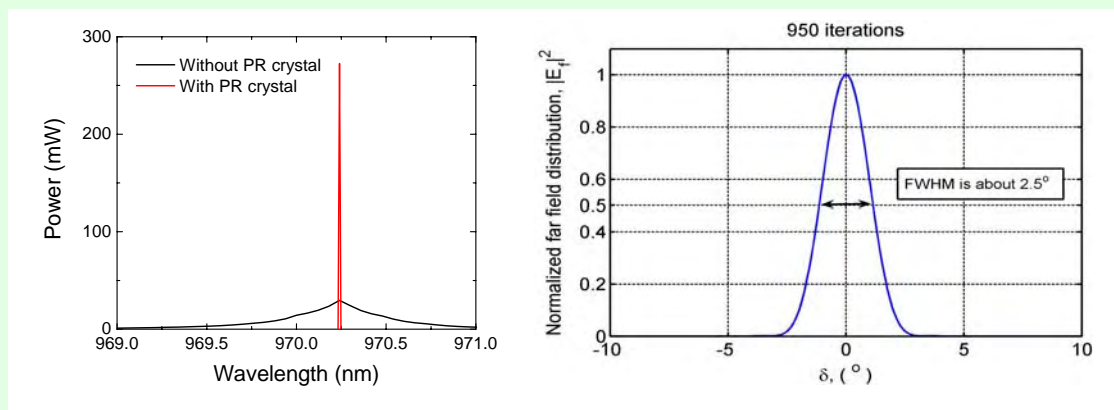
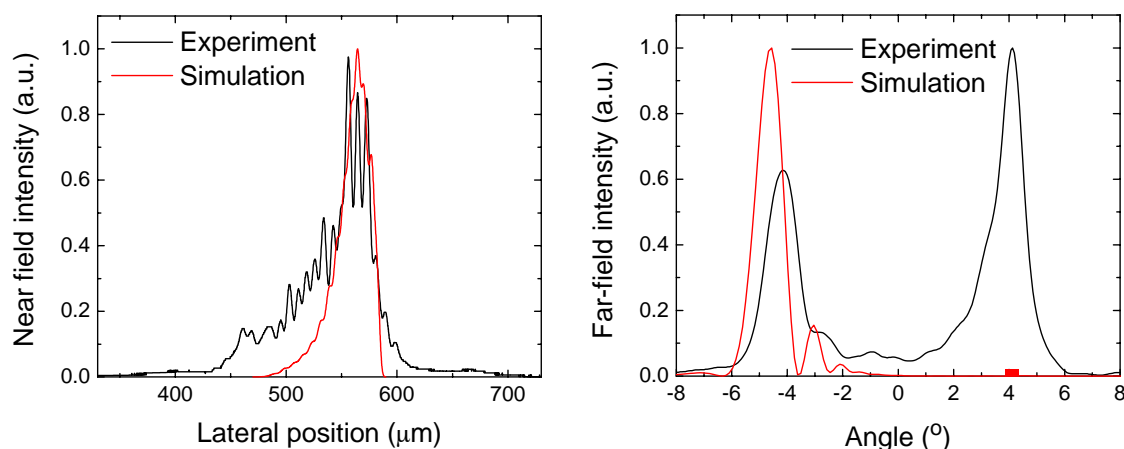


Figure 13: Calculated output spectra for the laser with and without a PR crystal inserted in the external cavity (left) and calculated far-field profile for the laser with a PR crystal in the external cavity (right).

Another example of an external cavity laser diode simulation being considered within BRIGHTER is that of a broad-area laser with asymmetric feedback [14]. The laser diode model uses the wide-angle finite difference beam propagation method (WA FD-BPM) with temperature- and carrier-induced lensing [15], while the external optics is modelled using the plane wave approach. The asymmetric feedback was experimentally demonstrated to offer significant improvement of the output beam of a broad-area laser [16]. The output of a broad-area laser is a superposition of a series of lateral modes. The purpose of using the asymmetric feedback is to selectively reflect one of the lateral modes back into the laser cavity, so that a stable beam is obtained. When the mirror is not placed at an appropriate position, the laser diode model does not converge due to lateral mode competition (mode partition noise). However, when the proper asymmetric feedback condition is chosen, the simulation becomes stable and shows a dramatic improvement of the beam quality.



**Figure 14: Converged near-field (left) and far-field (right) patterns of an asymmetric feedback external cavity laser. The mirror position and width are indicated by the red stripe in the plot of the far-fields.**

A series of simulations were made and a stable operating condition is found when a mirror stripe, 0.6 mm wide, is positioned 5.38 mm from the centre. The near-field pattern has an asymmetric shape as shown in Fig. 14 (left), in agreement with experiment. The far-field pattern shown in Fig. 14 (right) consists of a narrow main lobe with a FWHM of 1.1°, which is offset from the centre by ~4.6°. The experimental far-field profile shows a double lobed feature with both a significant output lobe (left) and feedback lobe (right). Such behaviour is uncommon for this asymmetric feedback technique. Usually, a strong and narrow output lobe is observed in the far-field, in agreement with the simulation, and the feedback lobe is strongly suppressed. The peculiar behaviour for this particular laser is not understood, but could be due to the presence of a windowed n-contact for this device. The absence of a lobe on the feedback side (with the mirror) of the simulated far-field profile could be due to the use of a perfect mirror reflectivity or the neglect of self-heating and current spreading effects in the simulations. Nevertheless, the position and width of the experimental lobe coincide well with the simulated profile.

## Summary

This article discusses several techniques developed in the WWW.BRIGHTER.EU project for improving the spatial and/or spectral brightness of laser diodes and bars. The approach chosen depends upon the beam properties required for a particular application. The techniques for the design and modelling of these external cavity lasers are also presented. The specific examples considered included self-organising external cavity lasers, laser bars with an external Talbot cavity, an external cavity laser bar with a wavelength multiplexed beam, and external cavity lasers with the asymmetric feedback.

## References

1. G. Pauliat, N. Dubreuil and G. Roosen, "Latest developments in photorefractive self-organized laser cavities," presented at Controlling Light with Light, OSA Topical Meeting, Lake Tahoe, USA, 14<sup>th</sup>-16<sup>th</sup> October 2007, Paper TuC7.
2. M. Chi, O. Bjarlin Jensen, J. Holm Lundemann, C. Pedersen, P.E. Andersen, G. Erbert, B. Sumpf and P.M. Petersen, "Tunable high-power narrow-linewidth semiconductor laser based on an external cavity tapered amplifier," *Optics Express* **13**, 10589-10596, (2005).
3. J. Holm Lundemann, O. Bjarlin Jensen, P.E. Andersen, S. Andersson-Engels, B. Sumpf, G. Erbert and P. M. Petersen, "High power 404 nm source based on second harmonic generation in PPKTP of a tapered external feedback diode laser," *Optics Express* **16**, 2486-2493, (2008).
4. R. Waarts, D. Mehuys, D. Nam, D. Welch, W. Streifer and D. Scifres, "High power, cw, diffraction-limited, GaAlAs laser diode array in an external Talbot cavity," *Applied Physics Letters* **58**, 2586-2588, (1991).
5. O. Efimov, L. Glebov, K. Richardson and V. Smirnov, "High-efficiency Bragg gratings in photothermorefractive glass," *Applied Optics* **38**, 619-627, (1999).
6. S. Yiou, F. Balembois, P. Georges and J.-P. Huignard, "Improvement of the spatial beam quality of laser sources with an intracavity Bragg grating," *Optics Letters* **28**, 242-244, (2003).
7. G. Venus, A. Sevian, V. Smirnov and L. Glebov, "High-brightness narrow-line laser diode source with volume Bragg-grating feedback," *SPIE Proceedings* **5711**, 166-176, (2005).
8. B. Volodin, S. Dolgy, E. Melnik, E. Downs, J. Shaw and V. Ban "Wavelength stabilization and spectrum narrowing of high-power multimode laser diodes and arrays by use of volume Bragg gratings," *Optics Letters* **29**, 1891-1894, (2004).
9. G. Lucas-Leclin, D. Paboeuf, P. Georges, J. Holm, P.E. Andersen, B. Sumpf and G. Erbert, "Wavelength stabilization of extended-cavity tapered lasers with volume Bragg grating," *Applied Physics B - Lasers and Optics* **91**, 493-498, (2008).
10. Z. Zhang, G. Pauliat, J.J. Lim, P.J. Bream, N. Dubreuil, A.J. Kent, E.C. Larkins and S. Sujecki, "Numerical modelling of high-power self-organizing external cavity lasers," in *Proceedings of the 8<sup>th</sup> International Conference on the Numerical Simulation of Optoelectronic Devices (NUSOD)*, Nottingham, U.K., 1<sup>st</sup>-5<sup>th</sup> September 2008, Paper MP18, submitted to *Optical and Quantum Electronics*, (2008).
11. P.J. Bream, J.J. Lim, S. Bull, A.V. Andrianov, S. Sujecki and E.C. Larkins, "The impact of a non-equilibrium gain in a spectral laser model," *Optical and Quantum Electronics* **38**, 1019-1027, (2006).
12. G. Pauliat, N. Dubreuil and G. Roosen, "Self-organizing laser cavities" in *Photorefractive materials and their applications 3: Applications*, P. Günter and J-P. Huignard (eds.), Springer Series in Optical Science, 253-275, (2007).
13. P.J. Bream, S. Sujecki and E.C. Larkins, "Investigation of nonequilibrium steady state gain in semiconductor quantum wells," *IEE Proceedings Optoelectronics* **153**, 299-307, (2006).
14. L. Lang, J.J. Lim, S. Sujecki and E.C. Larkins, "Improvement of the beam quality of a broad-area diode laser using asymmetric feedback from an external cavity," in *Proceedings of the 8<sup>th</sup> International Conference on the Numerical Simulation of Optoelectronic Devices (NUSOD)*, Nottingham, U.K., 1<sup>st</sup>-5<sup>th</sup> September 2008, Paper ThPD7, submitted to *Optical and Quantum Electronics*, (2008).
15. S. Sujecki, L. Borrueal, J. Wykes, P. Moreno, B. Sumpf, P. Sewell, H. Wenzel, T.M. Benson, G. Erbert, I. Esquivias and E.C. Larkins, "Nonlinear properties of tapered laser cavities," *IEEE Journal of Selected Topics in Quantum Electronics* **9**, 823-834, (2003).
16. B. Thestrup, M. Chi, B. Sass and P.M. Petersen, "High brightness laser source based on polarization coupling of two diode lasers with asymmetric feedback," *Applied Physics Letters* **82**, 680-682, (2003).

## Mirror Heating in High Power Lasers

Jens W. Tomm<sup>1</sup>, Mathias Ziegler<sup>1</sup>, Jose Manuel Garcia Tijero<sup>2</sup> and Ignacio Esquivias<sup>3</sup>

<sup>1</sup> Max-Born-Institut, Max-Born-Str. 2 A, 12489 Berlin, Germany.

<sup>2</sup> Dpto. Fisica Aplicada. E.T.S de Arquitectura. U.P.M. Ave. Juan de Herrera s/n. 28040 Madrid, España.

<sup>3</sup> Universidad Politecnica de Madrid, Dept. Tecnologia Fotonica, E.T.S.I. Telecomunicacion, Ciudad Universitaria, 28040 Madrid, España.

The optical feedback in edge-emitting semiconductor diode lasers originates from the partial reflection of the generated light at the front and rear facets. In high-power diode lasers, the facets experience very high optical and thermal loads, so that facet degradation represents a process that can potentially affect the reliability of the whole device. Sophisticated methods, such as the E2 technology developed at IBM Zürich (now Bookham), have been created for facet passivation and coating in order to limit facet degradation in single-mode emitters [1,2]. Nowadays, even laser bars consisting of broad-area (BA) emitters can reach comparable power densities when approaching the kW level and the front facet loads in these devices can exceed 120mW/μm [3]. Further developments of existing facet technology to such high power densities require an improved insight into the physics of facet degradation. This contribution attempts to provide some new material on this topic.

In this work, we study the dependence of front facet heating on the surface recombination velocity ( $s_v$ ) in BA single emitter devices. While  $s_v$  is determined by a novel two-colour time-resolved (TR) photoluminescence (PL) experiment, measured at the GaAs substrate part of the facet, the surface temperature is measured by micro-Raman ( $\mu$ R) spectroscopy directly from the waveguide area of the front facet of operating devices. The investigated devices have intentionally modified  $s_v$ -values. Although surface recombination is not the mechanism that directly causes catastrophic degradation, it is very likely to be a trigger for the associated destructive feedback loop [4] that eventually leads to the reliability limits of the present generation of high-brightness devices. Our two-colour TR-PL approach is considered a novel and versatile tool for the assessment of facet qualities and hence a benchmark for current and future passivation and coating technologies. Photographs of the experimental setups are shown in Fig. 1.

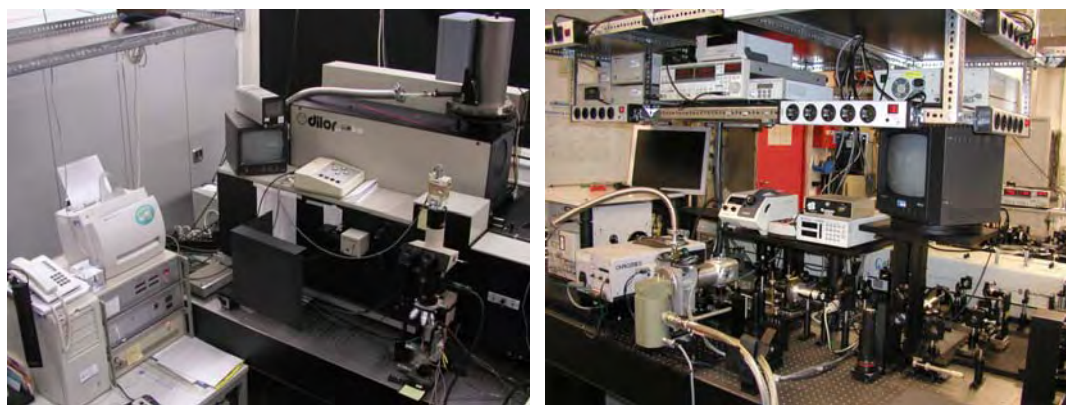


Figure 1: Photographs of the experimental setups:  $\mu$ R-spectrometer (left); TR-PL setup (right).

Laser structures designed for high-temperature operation at an emission wavelength of 808nm were grown by metal-organic vapour phase epitaxy on GaAs substrates by the BRIGHTER partner FBH. The semiconductor chips contain a 130μm wide laser stripe with a cavity length of 1500μm. Before applying a standard facet passivation / coating process, the surfaces were cleaned by irradiation with atomic hydrogen at elevated substrate temperatures as described in [5]. In this process, increasing substrate temperatures promote the sublimation of As out of the surface leaving defect sites behind. Thus, the substrate temperature is a parameter that allows for controlling the density of surface recombination centres and consequently tailoring the parameter  $s_v$ . The single emitter chips were soldered p-side down using AuSn onto CuW heat-spreaders, which are in turn attached to standard C-mounts. For these devices, the lasing thresholds are at about  $I=0.6A$  and the output power levels are about 4W at  $I=5A$ . The devices exhibit an uncritical thermal behaviour with a maximum output power of ~10W at 13.5A and a subsequent shut-down by thermal rollover.

Facets are measured by a  $\mu$ R technique in which temperatures are derived from the spectral shifts of TO phonon lines with an accuracy of approximately 10K. The 488nm line of an Ar-ion laser serves as the excitation source (excitation power  $\sim 850\mu\text{W}$ , spot diameter  $\varnothing_{1/e} \sim 1\mu\text{m}$ ) and illuminates the front facets in the range of the active region. Raman spectra were recorded with a DILOR x-y- $\mu$ R-spectrometer [1,6]. The samples were studied at stabilised heatsink temperatures of  $25.0^\circ\text{C} \pm 0.1^\circ\text{C}$  and injection currents of up to 2.25A.

Carrier lifetimes were derived from TR-PL measurements with two different excitation wavelengths ( $\lambda_{\text{ex}}$ ) of 790nm and 395nm. The excitation spot was located on the front facet in the range of the GaAs substrate. For  $\lambda_{\text{ex}}=790\text{nm}$  (absorption coefficient  $\alpha \sim 1.2 \times 10^4 \text{cm}^{-1}$ ), the penetration depth is in the range of microns and thus the PL originates mainly from the bulk of the devices, whereas the PL from a surface layer of several tens of nanometres thickness is detected with excitation at  $\lambda_{\text{ex}}=395\text{nm}$  ( $\alpha \sim 3 \times 10^5 \text{cm}^{-1}$ ). Analysis of the PL-transient ratios allows for the determination of  $s_p$ , while eliminating the influence of the bulk lifetime. The setup is based on a mode-locked Ti:sapphire laser (pulse duration  $< 100\text{fs}$ , repetition rate 82MHz, average excitation power  $\sim 10\text{mW}$ ) as the excitation source and a streak camera for TR-PL detection [1,7].

In Fig. 2, we present a schematic of the different heating mechanisms potentially contributing to the temperature rise of the facets as a function of injection current. The lasing threshold is set to be at unity. The heating due to surface recombination is governed by the magnitude of the recombination velocity  $s_p$  and saturates because of the finite number of surface states to be populated and/or the almost constant non-equilibrium-carrier concentration above the lasing threshold. In contrast, the contribution due to the re-absorption of laser emission starts approximately at the threshold. We include a phenomenological heating contribution proportional to the injection current. In general, the relative strength of the different contributions depends on the actual device structure and is not known *a priori*. Moreover, facet heating is an effect on top of the bulk heating, i.e. the measured facet temperatures involve all bulk heating effects.

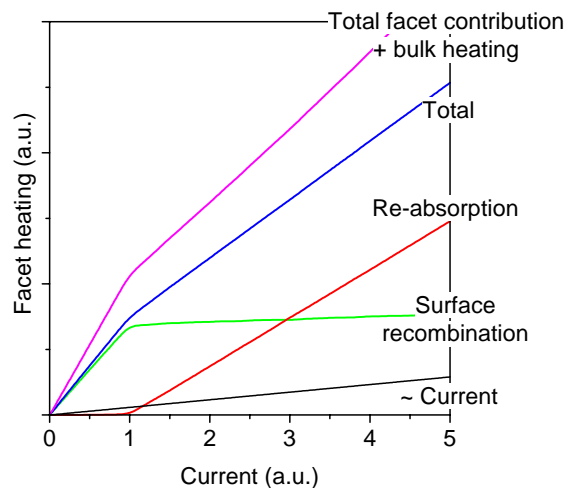


**Figure 2:** Heat contributions that potentially add to facet heating are plotted versus operation current. The lasing threshold is set to be at unity. The different contributions are marked. Note that the weighting factors that relate these contributions to each other are chosen arbitrarily, whereas the shape of each curve is given by the microscopic nature of the corresponding mechanism. For comparison with experimental facet temperatures, bulk heating effects have to be added, resulting in the transition from the blue line to the magenta line.

Experimentally determined temperatures of the active region within the bulk and at the facet for device A treated by hydrogen irradiation at a substrate heater temperature of  $400^\circ\text{C}$  and device B treated at a substrate heater temperature of  $550^\circ\text{C}$  are presented in Figs. 3 (a) and (b), respectively. The temperature increase  $\Delta T$  relative to the heatsink temperature is plotted as a function of the injection current. Red circles indicate the facet temperatures. When confining the analysis of the  $\mu$ R data to the range below the laser thresholds, we find average values  $\Delta T=4.0^\circ\text{C} \pm 1.5^\circ\text{C}$  and  $\Delta T=11^\circ\text{C} \pm 4^\circ\text{C}$  for devices A and B, respectively. The dashed lines give the measured electrical power,  $U \times I$ , and the full lines represent this power minus the optical output power  $P_{\text{opr}}$ , all multiplied by the average thermal resistance of the devices  $R_{\text{th}}=7.5\text{K/W}$ . The thermal resistance was determined in thermographic experiments [8]. Blue circles indicate the original thermographic data.

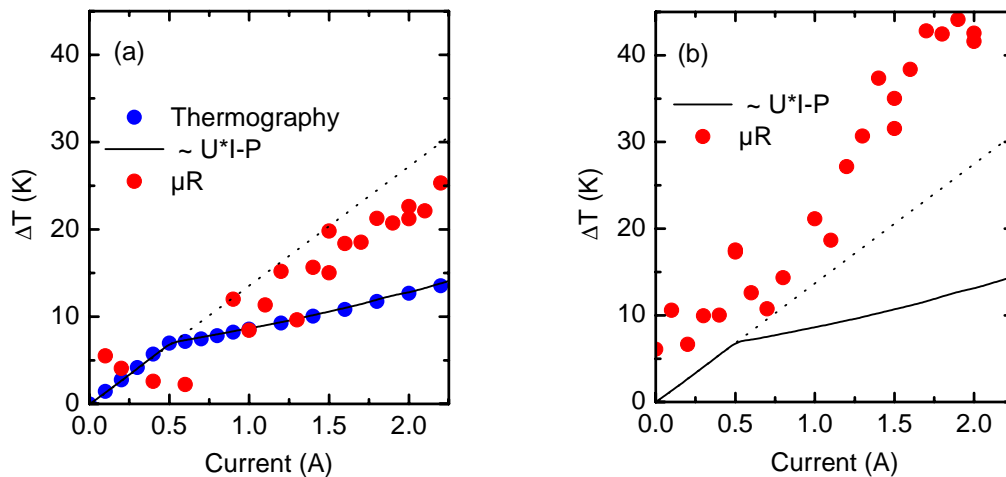


Figure 3: (a,b) Temperature increases above a heatsink temperature of 25°C for devices A and B, respectively. Bulk temperature increases are given by the black solid line, which is calculated as  $\Delta T_{bulk} = (U \times I - P_{opt}) R_{th}$ , and the black dotted line which is calculated as the upper limit for the bulk temperature of non-lasing devices from  $\Delta T = U \times I \times R_{th}$ . The thermal resistance ( $R_{th} = 7.5 \text{K/W}$ ) is derived from bulk temperature data which are independently obtained by thermography (see the blue circles in Fig. 3 (a)). Facet temperatures are marked by red circles. The dotted lines are guides to the eye in order to illustrate the facet temperature behaviour.

Results of the TR-PL experiments performed at the GaAs substrate part of the facet are summarised in Figs. 4 and 5. The decay of the PL signal after excitation at 790nm and at 395nm is plotted as a function of time in Fig. 4. In both devices, a faster decay is observed after excitation at 395nm, pointing to faster recombination kinetics after the excitation of a thin surface layer (395nm) compared to that of larger (bulk) volumes (790nm). To see this more clearly, we plot the ratio of the normalised PL-intensity transients measured with 395nm and 790nm excitation [ $I_{PL}(395\text{nm})/I_{PL}(790\text{nm})$ ] as a function of time for devices A (Fig. 5, full circles) and B (open circles). The data of Figs. 4 and 5 provide direct evidence that  $s_v$  in device B is substantially higher than in device A.

The lines in Fig. 5 are calculated from a rate equation model developed by Ahrenkiel [9,10]. One-dimensional rate equations for the time-dependent carrier concentration include bulk and surface recombination as well as a carrier diffusion term. These equations are solved analytically and spatially integrated over the non-equilibrium carrier-concentration profiles to derive a quantity proportional to the measured PL signal. In addition to the absorption coefficients given above, an ambipolar diffusion constant of  $3.3 \text{cm}^2/\text{s}$  is used, and the chart shown in Fig. 5 is obtained by varying the parameter  $s_v$ . A comparison the data points give values of  $s_v$  of  $<10^5 \text{cm/s}$  and of  $\sim 10^6 \text{cm/s}$  for the GaAs substrate part of the facets of devices A and B, respectively. This type of data analysis, as presented in Fig. 5, makes the resulting  $s_v$  values completely stable against fluctuations in the absolute PL signals and independent of the non-equilibrium carrier lifetime within the substrate.

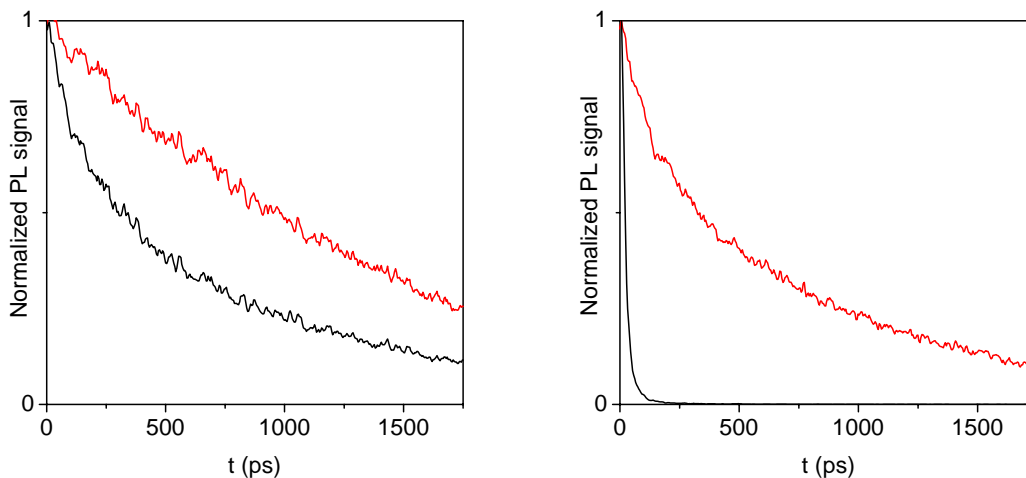


Figure 4: PL transients for devices A (left) and B (right) measured with excitation at  $\lambda_{ex} = 790\text{nm}$  (red lines) and 395nm (black lines). The spectrally integrated and normalised PL intensity is plotted as a function of time.

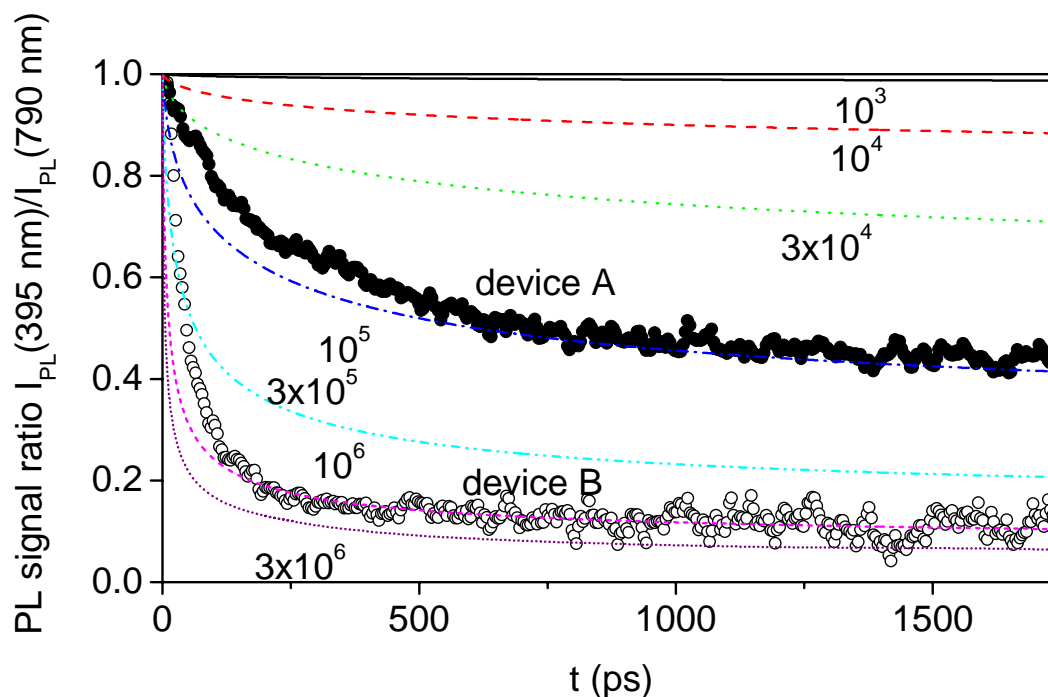


Figure 5: Ratios of PL intensities measured for device A (solid symbols) and B (open symbols) as a function of time. The fan chart of lines is calculated according to [9] with the parameter, from top to bottom,  $s_v=10^3$  cm/s (full),  $10^4$  cm/s (dashed line),  $3 \times 10^4$  cm/s (dotted line),  $10^5$  cm/s (dash-dotted line),  $3 \times 10^5$  cm/s (dash-dot-dotted line),  $10^6$  cm/s (short-dashed line) and  $3 \times 10^6$  cm/s (short-dotted line).

We start our discussion by recalling that the PL emission originates from the GaAs substrate part of the facet, whereas the  $\mu$ R facet temperatures are monitored at the active region part of the facet. Of course, a direct measurement of the QW PL would be more desirable, but fails due to interference from GaAs-related PL contributions. Therefore, we have to link either the methods or the locations at the facet, where the measurements were done:

- i. Given a comparable surface chemistry, the uniform treatment of the GaAs substrate part and the active region part of the facet is expected to cause similar tendencies regarding the creation of surface states. This should result in comparable tendencies with respect to  $s_v$ .
- ii. Although  $\mu$ R does not directly probe  $s_v$ , the impact of  $s_v$  on the facet temperature increase is largest below the lasing threshold (see our discussion of Fig. 2). Thus, we consider the average below threshold heating data of  $\Delta T=4.0^\circ\text{C} \pm 1.5^\circ\text{C}$  and  $\Delta T=11^\circ\text{C} \pm 4^\circ\text{C}$  for devices A and B, respectively, a strong indication that the  $s_v$  value at the active region of device A is lower than for device B. Hence, the results obtained by TR-PL, namely  $s_v < 10^5$  cm/s and  $s_v \sim 10^6$  cm/s for the GaAs substrate part of the facets of devices A and B are at least qualitatively confirmed for the active region as well.
- iii. A careful photocurrent analysis of both devices clearly points to a lower  $s_v$  value at the active region of device A as compared to device B. Because of the large number of parameters involved in complementary modelling, see for example [11], such results also do not provide values for  $s_v$  at the active region.

Because of these arguments, we are convinced that an extension of the tendencies observed at the GaAs part of the facets towards the active region part of them is justified. In turn, we have to admit that the specific values for  $s_v$  of  $< 10^5$  cm/s and  $\sim 10^6$  cm/s for devices A and B, respectively, hold for the GaAs part of the facets only and not automatically for the active region. Furthermore, for completely different device architectures, where the surface chemistry of the substrate and active region greatly differ, this approach may fail.

Extending our discussion to the above threshold range, we find the bulk temperatures of devices A and B to be almost the same. The facet temperatures, however, are strikingly different. Device A displays a moderate increase of facet temperature with current, exceeding the bulk temperature by at most 10K in the current range shown. For device B, this increase amounts to 30K and also a steeper change of the slope takes place at the threshold. Such a change is interpreted as a change of the governing heating mechanism. Since the heating due to surface recombination saturates not later than at the lasing threshold, only re-absorption might explain such an increase of the slope beyond threshold (see discussion on facet heating mechanisms in Fig. 2). Thus, it is likely that what is observed here is the transition from surface recombination to re-absorption as the dominant heating mechanism. This leads us to the insight that increased surface recombination is accompanied by increased re-absorption. In principle, the microscopic nature of defects giving rise to enhanced surface recombination and reabsorption heating could be different but - if existing - both types originate from the different facet preparation applied.

In summary, we have combined micro-Raman and time-resolved photoluminescence studies to correlate surface recombination velocities, near-facet defect densities and surface temperatures of the front facets of 808nm emitting broad-area laser devices. Analyses of devices with tailored surface properties show clearly that increased surface recombination velocities are accompanied by increased facet temperatures. Furthermore, we show that poorer surface properties result in enhanced facet heating caused by reabsorption of the laser light. Our approach is considered a versatile tool for the assessment of facet quality, provided that the surface chemistry of substrate and active region do not greatly differ.

#### ACKNOWLEDGEMENTS

Expert technical assistance by Sandy Schwirzke-Schaaf and Tobias Grunske is gratefully acknowledged. The devices were fabricated by the BRIGHTER partner Ferdinand-Braun-Institut für Höchstfrequenztechnik, Berlin (FBH) and placed at our disposal by Götz Erbert and Frank Bugge.

#### REFERENCES

1. A. Oosenbrug and E.E. Latta, "High-Power Operational Stability of 980 nm Pump Lasers for EDFA Applications", LEOS Annual Meeting 1994, Boston, MA, paper DL1.2, (1994).
2. M. Gasser and E.E. Latta, "Method for Mirror Passivation of Semiconductor Laser Diodes," U.S. Patent 5144634, Sep. 1, 1992.
3. H. Li, T. Towe, I. Chyr, D. Brown, T. Nguyen, F. Reinhardt, X.R. Srinivasan, M. Berube, T. Truchan, R. Bullock and J. Harrison, "Near 1 kW of Continuous-Wave Power From a Single High-Efficiency Diode-Laser Bar", IEEE Photon. Technol. Lett. 19, 960 (2007).
4. G. Chen and C.L. Tien, "Facet heating of quantum well lasers", J. Appl. Phys. 74, 2167 (1993)
5. P. Ressel, G. Erbert, U. Zeimer, K. Häusler, G. Beister, B. Sumpf, A. Klehr and G. Tränkle, "Novel passivation process for the mirror facets of Al-free active-region high-power semiconductor diode lasers", IEEE Photon. Technol. Lett. 17, 962 (2005).
6. J.W. Tomm, E. Thamm, A. Bärwolff, T. Elsaesser, J. Luft, M. Baeumler, S. Mueller, W. Jantz, I. Rechenberg and G. Erbert, "Facet degradation of high-power diode laser arrays", Appl. Phys. A 70, 377 (2000).
7. V.G. Talalaev, J.W. Tomm, N.D. Zakharov, P. Werner, B.V. Novikov and A.A. Tonkikh, "Transient spectroscopy of InAs quantum dot molecules", Appl. Phys. Lett. 85, 284 (2004).
8. M. Ziegler, F. Weik, J.W. Tomm, T. Elsaesser, W. Nakwaski, R.P. Sarzała, D. Lorenzen, J. Meusel and A. Kozłowska, "Transient thermal properties of high-power diode laser bars", Appl. Phys. Lett. 89, 263506 (2006).
9. R.K. Ahrenkiel, Current Topics in Photovoltaics 3, 1 (1988).
10. R.K. Ahrenkiel, "Minority-Carrier Lifetime in III-V Semiconductors", Semiconductors and Semimetals, vol. 39, Academic Press, Inc., pp. 39-150, (1993).
11. J.W. Tomm, A. Bärwolff, U. Menzel, M. Voß, R. Puchert, T. Elsaesser, F.X. Daiminger, S. Heinemann and J. Luft, "Monitoring of aging properties of AlGaAs high-power laser arrays", J. Appl. Phys. 81, 2059 (1997).

## High-Brightness Tapered Lasers with Multiple Contacts

P. Adamiec, K.-H. Hasler, H. Wenzel, B. Sumpf, G. Erbert

*Ferdinand-Braun-Institut für Höchstfrequenztechnik, Gustav-Kirchhoff-Str. 4, 12489 Berlin, GERMANY*

### Introduction

Nowadays, due to compactness, high conversion efficiency, and low cost, semiconductor lasers have become more and more important sources in different application fields like communications, data storage, medicine and entertainment. There are some particular applications which require high power combined with nearly diffraction limited beam quality. These include efficient coupling into optical fibres or into crystals for non-linear frequency conversion, optical wireless communications and laser display applications. The latter two applications also require high frequency modulation of the output power. The most promising type of diode laser to meet all of the mentioned demands is a tapered laser consisting of a straight ridge waveguide section and a tapered amplifying part [1], each of which can be individually controlled.

### Application requirements

Optical wireless communication systems are used to transmit data in free atmosphere, typically for short range outdoor systems with high data rate intra-building networking applications. They deliver transmission rates in the range of 100 Mbps up to 2.5 Gbps. As transmitters, near infra-red (NIR) high-brightness lasers emitting in atmospheric windows are required. They should have the capability of high speed modulation and output powers in the Watt-range.

Laser display projection systems provide more realistic, natural colour gamut on a projection screen by using red, green, and blue laser sources. Flying spot projection displays require high brightness lasers because the pixel size on the screen is defined by the laser spot size. Moreover, high frequency amplitude modulation in the 100 MHz range is required. Diode lasers emitting in the red and blue spectral range with the necessary output power and beam quality are under development. For the emission in the green, the most promising attempt is the frequency doubling (second harmonic generation - SHG) of NIR semiconductor lasers. For flying spot projection displays, the laser sources should deliver a reliable output power of about 500 mW with nearly diffraction limited beam quality. For the diode lasers in the NIR spectral region used as excitation sources for the SHG and assuming a typical conversion efficiency of about 15%, a reliable output power of about 3 W is necessary. Due to the spectral acceptance bandwidth of the SHG crystal being about 0.2 nm, the NIR diode lasers should have a narrow spectral linewidth below this value and should operate at a constant wavelength during modulation.

### Devices – State-of-the-art

Compared to longer wavelength devices, the major challenge for the design of 650 nm devices is the poor confinement of electrons and holes in the active layer due to low energy barriers. This leads to a low wall-plug efficiency and a high temperature sensitivity. The majority of the laser structures for this spectral range are based on one or more InGaP quantum wells as the active layer embedded in AlGaInP waveguide and AlInP cladding layers. These layer structures typically result in vertical far field angles above 42° (full-width at half maximum - FWHM) and require AlInP processing.

At 650 nm, reliable operation at 50 mW and 60°C of a narrow stripe width laser with window-mirror laser diodes was reported by Shima *et al.* [2]. Using a two step epitaxy and a sophisticated laser structure at 659 nm, Onishi *et al.* [3] reported a maximum output power of 150 mW (100 ns pulses, 50% duty cycle) from 2.5 µm RW lasers.

Broad area lasers for 650 nm were recently reported by our group. A maximum output power of 3 W with conversion efficiencies up to 40% were reported [4]. These devices showed reliable operation over 10,000 h at 1 W output power [5].

Tapered lasers at 635 nm were reported by Pezeshki *et al.* [6]. These devices reached a maximum output power of 600 mW. Up to an output power of 400 mW, the beam quality was diffraction limited. 900 mW of output power from a tapered laser at 640 nm was reported by Linder *et al.* [7]. At 700 mW, a beam propagation ratio  $M^2 \approx 3$  was achieved. Recently, our group reported, for common contact devices mounted on diamond heat-spreaders, a maximum output power of 1 W and a reliable operation over 2000 h at 500 mW [8].

In the case of the 1060 nm devices, the necessary small spectral linewidth can be achieved by using distributed Bragg reflector (DBR) or distributed feedback (DFB) lasers. At  $\lambda \approx 1065$  nm, Achtenhagen *et al.* [9] reported an output power of 700 mW. Output powers up to 300 mW were obtained with a monolithically integrated ridge-waveguide (RW) master-oscillator power-amplifier (MOPA) by Brox *et al.* [10], where the emission wavelength changed about 160 pm when changing the injection current.

To reach a higher output power, hybrid MOPA systems can be used where the emission of a master oscillator, e.g. a DBR or DFB laser as mentioned above, is amplified in strongly anti-reflection coated broad area or tapered devices. The latter typically consist of a straight RW section and a tapered section. At 1080 nm, our group reported an output power up to 7.4 W [11]. A more compact system with a maximum power of 3.1 W at 1060 nm was reported by Schwertfeger *et al.* [12].

Monolithically integrated semiconductor lasers, based on devices with internal gratings and a flared amplifier are known for several wavelengths. For the wavelength range between 970 nm and 980 nm, an output power of 12 W from a DBR tapered laser utilizing a 6<sup>th</sup> order surface grating was reported by Fiebig *et al.* [13]. For the same wavelength range, 10 W of output power was reached with a monolithically integrated flared MOPA using a second order grating for the DBRs buried into the layer structure by a sophisticated two-step epitaxy [14].

In this article, twin-contact tapered lasers at 650 nm and 1060 nm will be presented. The vertical layer structures, the lateral design, the independent control of ridge waveguide and tapered section and the adapted mounting scheme are all presented. For the 1060 nm DBR tapered laser, the design of the deeply etched 6<sup>th</sup> order grating is given. The basic data of our laser structures is also shown. Experimental results are given for lasers mounted p-side down on AlN submounts with twin-contacts, which allow independent control of the RW and taper sections.

## 650 nm tapered lasers

Due to the lower energetic barriers for electrons and holes between the active region and surrounding layers a careful development of the epitaxial layer structure is necessary. To reach nearly diffraction limited beam quality at higher output powers, attention must be paid to the lateral layout design.

### Sample description

A 20 nm InGaP single quantum well (QW) was chosen as the active layer, which was embedded in AlGaInP waveguide layers. Whereas the n-cladding layer is formed by AlInP, the p-cladding is formed by AlGaAs, which allows carbon p-type doping with concentrations larger than  $10^{18}$  cm<sup>-3</sup>. The vertical far field angle at full width at half maximum (FWHM) is only 31° (or 54°, when including 95% of the emitted power). This is comparable to our previously published structure [8] and substantially smaller than other reported values [15].

Characteristic data of the laser structure have been obtained from pulsed (1  $\mu$ s, 1 kHz) measurements of uncoated 1 mm long broad area lasers with 100  $\mu$ m stripe width. The threshold current is  $I_{th} = 600$  mA, the differential efficiency  $\eta_D = 0.81$ , and the characteristic temperature  $T_0 = 65$  K. From the analysis of lasers with different lengths, assuming a logarithmic dependence of the modal gain on current density, the following quantities have been obtained: internal losses  $\alpha_i = 1.9$  cm<sup>-1</sup>, internal efficiency  $\eta_i = 0.97$ , modal gain factor  $\Gamma g_0 = 34$  cm<sup>-1</sup>, and transparency current density  $j_{tr} = 404$  A/cm<sup>2</sup>. The significant improvement in the internal efficiency and characteristic temperature of the threshold current  $T_0$  in comparison to the previously published structure ( $\eta_i = 0.82$  and  $T_0 = 55$  K) used for tapered laser fabrication [8] can be attributed to the replacement of the 5 nm thin compressively-strained QW by a 20 nm thick tensile-strained QW.

The tapered lasers have a 2 mm long resonator with a 750  $\mu$ m RW and a 1250  $\mu$ m tapered section. The ridge waveguides with a width of 3  $\mu$ m were manufactured using reactive ion etching. The contact window of the tapered section was defined by ion implantation. The full taper angle is 4°. The laser facets were coated with mirrors reflectivities of 1% and 96% for the front and rear facets, respectively. A passivation process was performed at both facets [16]. The lasers were soldered p-side down using AuSn on AlN submounts with separated contacts, which allows the independent control of both taper and RW currents. The coefficient of thermal expansion (CTE) for AlN is  $CTE = 4.3 \cdot 10^{-6}$  K<sup>-1</sup>. This is close to the value for GaAs ( $CTE = 6.4 \cdot 10^{-6}$  K<sup>-1</sup>). The thermal conductivity of 180 W·m<sup>-1</sup>·K<sup>-1</sup>, which is comparable to CuW (the usual submount material for AuSn soldering), and the large specific resistance of  $1 \times 10^{11}$   $\Omega$ ·m allows the use of structured submounts. The AlN subassembly was soldered with SnAgCu to a conductively cooled package with a footprint of 25x25 mm<sup>2</sup>.

### Experimental results

Figure 1 shows the dependence of the output power  $P$  on the taper current  $I_{taper}$  for different RW currents  $I_{RW}$ . The taper current necessary to start the laser action decreases with increasing RW current. The device started lasing at  $I_{taper} = 0.37$  A for  $I_{RW} = 50$  mA and the threshold current  $I_{th} = I_{RW} + I_{taper}$  was 0.42 A. The slope efficiency determined at lower power (up to 200 mW) was 0.82 W/A. An output power of 515 mW was reached at  $I_{taper} = 1.2$  A. A maximum conversion efficiency  $\eta_C = 16\%$  was obtained, which is 2% higher than the conversion efficiency obtained for devices from a previous epitaxial layer structure mounted on diamond [8]. The threshold currents, slope and conversion efficiencies for other RW currents are compiled in Table 1.

An optical spectrum taken at 500 mW output power is given in Fig.2. The peak wavelength was 645.7 nm and the full width at half maximum was 160 pm.

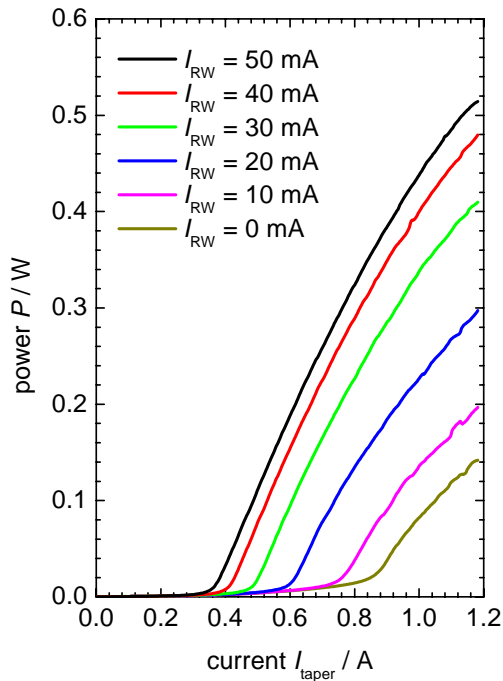


Fig. 1: Output power versus taper current for different RW currents taken at 15°C.

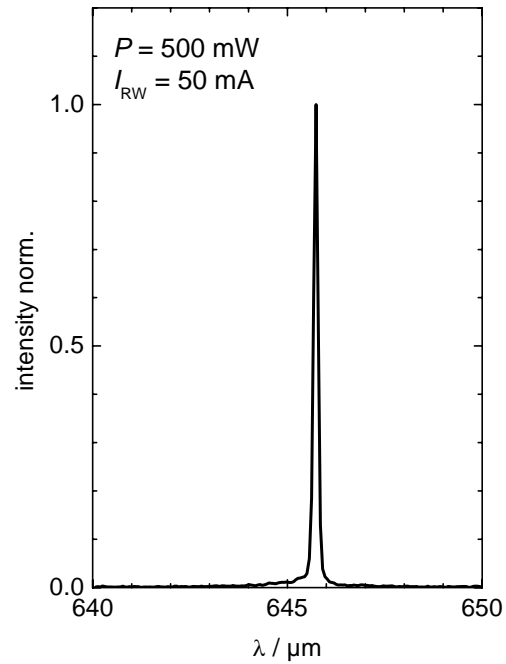


Fig. 2: Optical spectrum at an output power of 500 mW measured at 15°C.

Lateral beam waist and far field profiles measured at fixed  $I_{RW} = 50$  mA and an output power of about 500 mW are shown in Fig. 3. A pronounced central lobe with 82% of the total power, i.e. 410 mW, can be seen. The width of the beam waist increases from 5.5  $\mu\text{m}$  to 7.2  $\mu\text{m}$ , whereas the far field angle decreases from 10.7° to 6.9°, when the power increases from 100 mW to 500 mW (see Table 2). Aforementioned values of beam waist and far field were measured at the  $1/e^2$  level and yield a beam quality factor of  $M^2 = 1.1$  for 500 mW output power. The astigmatism changes by about 140  $\mu\text{m}$  with increasing power.

$I_{RW}$ (mA)	$I_{th}$ (mA)	$S$ (W/A)	$\eta_{C \max}$
0	0.885	0.48	0.04
10	0.765	0.47	0.06
20	0.630	0.61	0.10
30	0.515	0.74	0.13
40	0.460	0.81	0.15
50	0.420	0.82	0.16

Table 1: Threshold currents  $I_{th}$ , slope efficiencies  $S$ , and conversion efficiencies  $\eta_{C \max}$  for different RW currents  $I_{RW}$ .

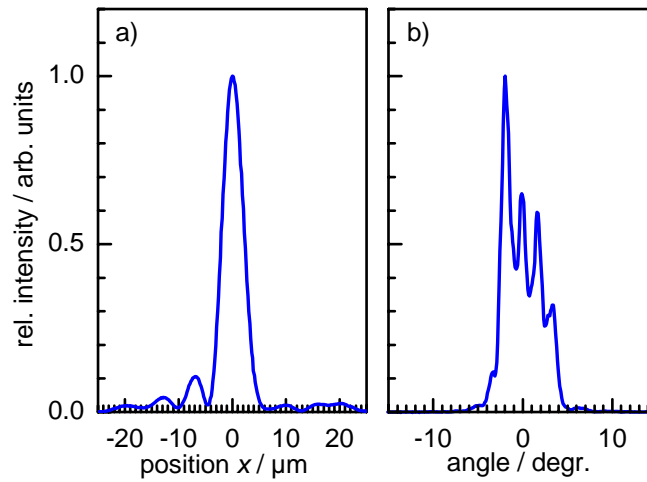


Fig. 3: Lateral profiles of the beam waist (a) and the far field (b) taken at  $I_{RW} = 50$  mA and output power of 500 mW. Measurements done at 15°C.

$P$ (mW)	$BW$ ( $\mu\text{m}$ )	$\theta_{FF}$ ( $^\circ$ )	$NF$ ( $\mu\text{m}$ )	$M^2$ ( $1/e^2$ )	$P_{c.l.}$ (%)	Astigm. ( $\mu\text{m}$ )
100	5.5	10.7	79	1.3	87	420
250	9.6	9.4	76	1.9	81	480
500	7.2	6.9	75	1.1	82	560

Table 2: Beam parameters measured at  $I_{RW} = 50$  mA and different power levels at 15°C,  $BW$  – beam waist,  $\theta_{FF}$  – lateral far field,  $NF$  – near field,  $M^2(1/e^2)$  –  $M^2$  at the intensity level at  $1/e^2$ ,  $P_{c.l.}$  – power in central lobe, Astigm. – astigmatism.

Figure 4 shows the variation of beam waist width and far field angle with increasing RW current measured at a fixed taper current ( $I_{taper} = 1.2$  A). It can be seen that the beam waist width remains constant with increasing RW current. This behaviour confirms that only the fundamental mode is injected from the RW section into the tapered part of the laser. The far field angle decreases slightly with increasing RW current. The astigmatism changes by about 130  $\mu\text{m}$  with the variation of RW current.

In summary, the device performance of tapered lasers with a 20 nm thick QW is improved compared to devices with a 5 nm QW. Careful design of the lateral layout allows one to reach 500 mW of output power together with nearly diffraction limited beam quality, as required for laser display applications. Moreover, AlN mounts with twin-contacts allow independent control of the RW and tapered sections and offer the possibility of high frequency modulation.

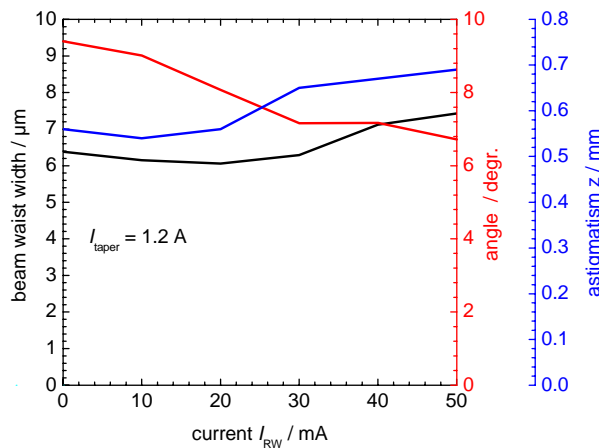


Fig. 4: Dependence of the beam waist width (black line), far field angle (red line), and astigmatism (blue line) on the RW current at fixed taper current  $I_{taper} = 1.2$  A.

## 1060 nm DBR-tapered lasers

The small spectral linewidth, which is necessary for SHG for the laser display application can be achieved by using distributed Bragg reflector (DBR) or distributed feedback (DFB) lasers. Since single-section high-power DFB lasers suffer from a strong thermally induced wavelength shift under current modulation, they are not suited for SHG for display technology. Therefore, to ensure a small spectral linewidth a single passive DBR was introduced in the RW section of the tapered laser. Thus, the DBR acts as the rear mirror of the laser cavity.

### Basic characteristic data of layer structure

The layer structure grown by metal-organic vapour phase epitaxy contains an InGaAs triple quantum well (TQW) active region embedded in a 4.8  $\mu\text{m}$  broad  $\text{Al}_{0.25}\text{Ga}_{0.75}\text{As}/\text{Al}_{0.35}\text{Ga}_{0.65}\text{As}$  super large optical cavity and results in a narrow vertical divergence of  $15^\circ$  (FWHM) and  $25^\circ$  including 95% of the emitted power. A TQW was chosen to compensate the reduction of the overlap of the optical field with the active region. The basic characteristic data was determined in the same way as described for the 650 nm laser structure: threshold current  $I_{th} = 296$  mA, the differential efficiency  $\eta_D = 0.85$  and the characteristic temperature  $T_0 = 149$  K. From the analysis of lasers with different lengths, the following quantities were obtained: internal losses  $\alpha_i = 1.1$   $\text{cm}^{-1}$ , internal efficiency  $\eta_i = 0.97$ , modal gain factor  $\Gamma g_0 = 27$   $\text{cm}^{-1}$ , and transparency current density  $j_{tr} = 191$  A/cm<sup>2</sup>.

### Design and fabrication of DBR tapered lasers – Sample description

The reflectivity of Bragg gratings decreases strongly with their order. However, for deeply etched gratings the reflectivity can be very high if the duty cycle is chosen carefully. The duty cycle is the ratio between length of the unetched region and the grating period. The reflectivity spectra of a 1 mm long DBR with a 6<sup>th</sup> order surface grating were calculated with the CAMFR (CAvity Modelling FRamework) tool [17] for defined duty cycles and the results are presented in Fig. 5 as a 2D-intensity plot. The maximum reflectivity decreases strongly with decreasing duty cycle of the grating. Therefore, one crucial point of the technology chosen (deep etching) is the adjustment of a sufficiently large duty cycle larger than 0.80 in order to obtain a reflectivity of the DBR of more than 20%.

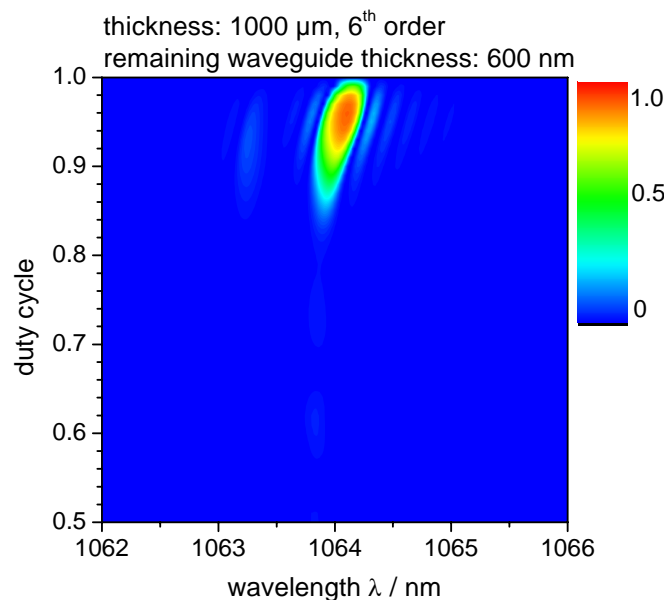


Fig. 5: Simulation of the reflectivity of a 6<sup>th</sup> order DBR-grating for 1060 nm for different duty cycles.

The 6<sup>th</sup> order Bragg grating with a period of about 1  $\mu\text{m}$  and the RW were simultaneously etched into the p-contact, p-cladding and a part of the p-confinement layer by reactive ion etching (see Fig. 6). Further details can be found in Ref. [18]. The contact window for the gain guided tapered section was defined by ion implantation. The front facet was coated to  $R_f = 1\%$ , whereas the rear facet (grating side) was coated to less than 0.1%. The small reflectivity of the rear facet was chosen in order to suppress parasitic reflections. The achievement of a very low value is not critical for the device performance. Both facets were passivated [16].

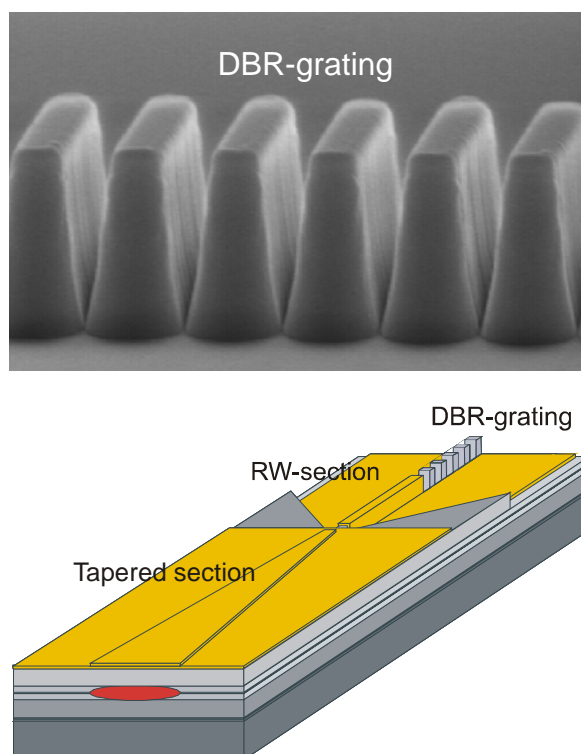


Fig. 6: DBR-grating (top) and schematic diagram of the DBR tapered laser (bottom).

The DBR tapered laser presented here has a total length of 4 mm. The passive DBR section located at the rear end and the active RW gain section both have a length of 1 mm. The RW width and taper angle are 4  $\mu\text{m}$  and 6°, respectively. A reflectivity of about 30% of the DBR was estimated by measuring the output power from the front and the rear facets of a DBR RW laser with the same section lengths (but with a straight instead of a tapered section) and identical facet reflectivities from the same wafer. This corresponds to an effective duty cycle of about 0.84 (see Fig. 5). The device was mounted p-side down on AlN submounts with twin-contacts using AuSn. This subassembly was soldered on a conduction cooled package with a footprint of 25x25 mm<sup>2</sup>.

## Experimental results

The dependence of the output power  $P$  on the taper current  $I_{\text{taper}}$  for different RW currents  $I_{\text{RW}}$  is shown in Fig. 7. The taper current necessary for starting laser operation decreases with increasing RW current. For  $I_{\text{RW}} = 300$  mA, the device starts lasing at  $I_{\text{taper}} = 0.61$  A (threshold current  $I_{\text{th}} = I_{\text{RW}} + I_{\text{taper}} = 0.91$  A) and the slope efficiency is  $S = 0.8$  W/A for  $P < 2$  W. This relatively low slope efficiency is due to scattering losses typical for a tapered laser and due to the low rear DBR reflectivity. The maximum conversion efficiency (not shown here) reaches about 35%. For larger taper currents, the slope decreases and the kinks in the characteristics caused by the thermal detuning of the gain and DBR sections become more and more pronounced. The output power increases with increasing RW current up to the largest chosen value of  $I_{\text{RW}} = 450$  mA, where a maximum power of 5.2 W was obtained for a taper current of 8.9 A.

An optical spectrum measured at  $P = 5$  W and  $I_{\text{RW}} = 300$  mA is shown in Fig. 8. The peak wavelength is 1062.8 nm and 95% of the emitted power is within a spectral width of 40 pm. The resolution bandwidth of the optical spectrum analyser was 14 pm.

The beam waist and far field profiles at an output power of 5 W and fixed  $I_{\text{RW}} = 300$  mA are shown in Fig. 9. The beam waist profile consists of a well pronounced central lobe with 72% of the total power, i.e. 3.6 W. The width of the beam waist increases from 6.8  $\mu\text{m}$  to 13.8  $\mu\text{m}$  and the far field angle decreases from 13.7° to 11.4° when the power is increased from 1 W to 5 W (see Table 3). At  $P = 5$  W, these values were determined at the  $1/e^2$  level and yield a beam quality factor of  $M^2 = 2$ . The astigmatism remains within the range between 700  $\mu\text{m}$  and 800  $\mu\text{m}$  and can thus be readily compensated by a cylindrical lens in the focusing optics [19].

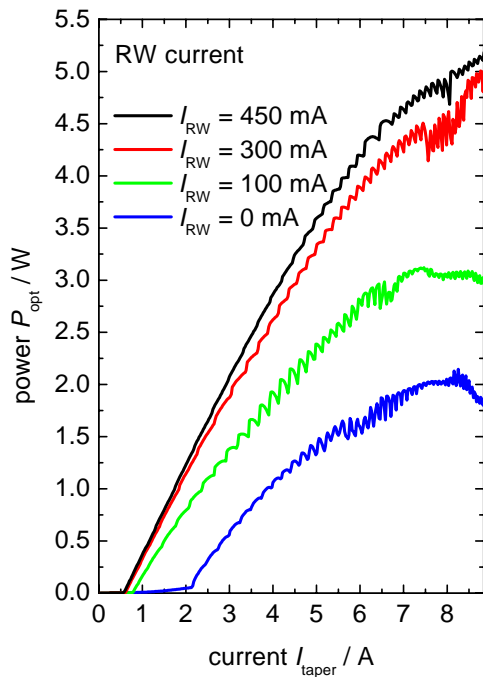


Fig. 7: Output power versus taper current for different RW currents taken at 25°C.

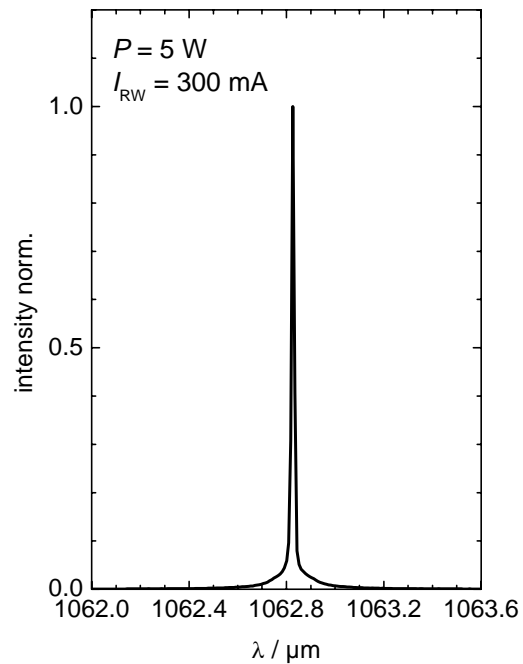


Fig. 8: Optical spectrum at an output power of 5 W measured at 25°C.

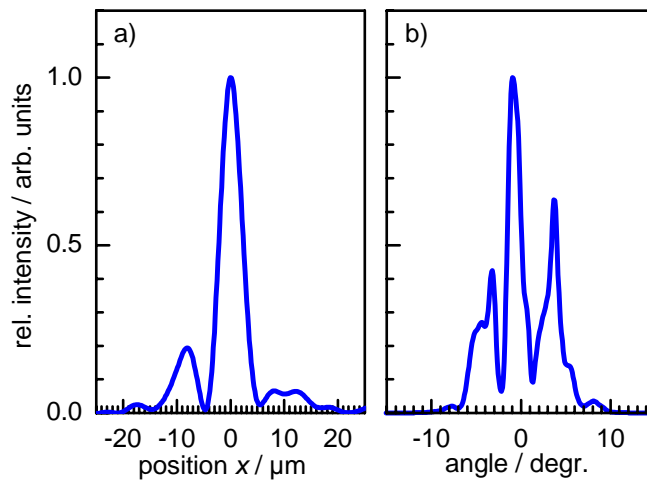


Fig. 9: Lateral profiles of the beam waist (a) and the far field (b) taken at  $I_{RW} = 300$  mA and an output power of 5 W. Measurements done at 25°C.

$P$ (W)	BW ( $\mu\text{m}$ )	$\theta_{FF}$ ( $^\circ$ )	NF ( $\mu\text{m}$ )	$M^2$ ( $1/e^2$ )	$P_{c.l.}$ (%)	Astigm. ( $\mu\text{m}$ )
1	6.8	13.7	174	1.2	90	700
2	6.8	15.5	182	1.4	81	750
3	11.7	14.3	173	2.2	72	770
4	12.0	12.2	164	1.9	73	800
5	13.8	11.4	137	2.0	72	770

Table 3: Beam parameters measured at  $I_{RW} = 300$  mA and different power levels at 25°C, BW – beam waist,  $\theta_{FF}$  – lateral far field, NF – near field,  $M^2(1/e^2)$  –  $M^2$  at the intensity level at  $1/e^2$ ,  $P_{c.l.}$  – power in central lobe, Astigm. – astigmatism.

Figure 10a shows a mapping of optical emission spectra versus RW current measured at a taper current  $I_{taper} = 2.25$  A. It can be seen that the emission wavelength remains almost constant at  $\lambda = 1061.8$  nm. The emission bandwidth of only 130 pm is in the range of the typical acceptance width of SHG crystals. Thus, the device is suitable as a pump source for the generation of green light ( $\lambda \sim 530$  nm). As seen in Fig. 10b, the output power rises from 0.17 W to 1.5 W when  $I_{RW}$  is increased from 0 to 450 mA. This allows high frequency modulation of the pump and SHG power with a large extinction ratio.

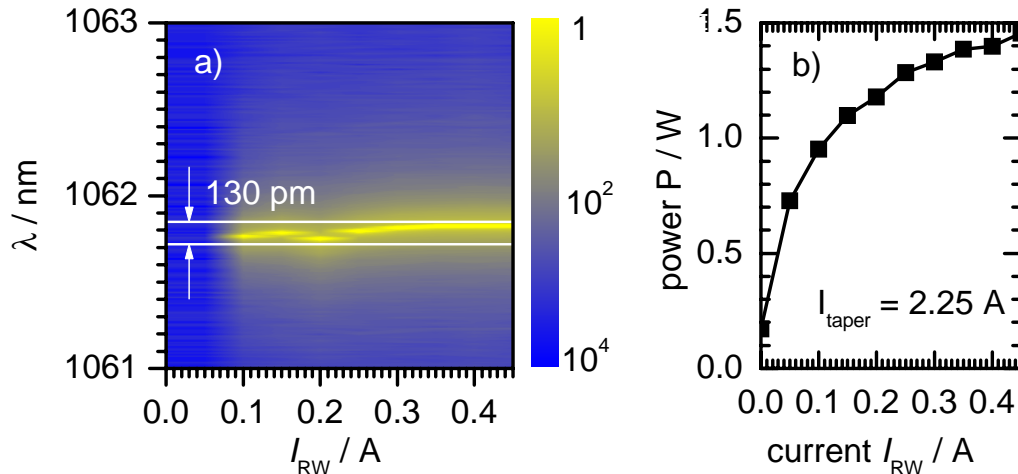


Fig. 10: (a) Colour-scale plot of the optical spectra vs. RW current. Yellow (light) - high intensity, blue (dark) - low intensity. (b) Corresponding output power. The taper current is  $I_{taper} = 2.25$  A.

In summary, the implementation of the DBR grating allows for operation at almost constant wavelength during modulation. Additionally, the high output power of about 5 W with nearly diffraction limited beam quality ensures that devices are suitable as light sources for SHG. Since they are mounted on an AlN submounts with twin-contacts, the RW and tapered sections can be independently controlled. Thus, the lasers are suitable for laser display applications or optical wireless communications.

## Conclusion

In this paper, tapered lasers emitting at 650 nm and DBR tapered lasers emitting at 1060 nm were presented. The devices were mounted on AlN submounts with separated contacts, which allows for independent control of the RW and tapered sections. The RW section was operated with small currents and the tapered section was operated with a high continuous wave (CW) current. This operational mode led to a decreased variation of the device temperature, caused by the self heating. Indeed, careful design of the laser structure for red lasers led to the improvement of the device performance. In case of devices emitting at 1060 nm, the implementation of a 6<sup>th</sup> order DBR as a rear mirror allows operation at almost constant wavelength during the variation of the RW current. Due to easy (single step) processing, this approach seems to be promising for large scale production.

## Acknowledgment

The authors acknowledge the technical support of P. Brade, A. Krause, A. Müller, R. Olschewski, and S. Wiechmann. This work was supported by the European Commission through the IST research project WWW.BRIGHTER.EU (IST-035266).

## References

1. J. N. Walpole, "Semiconductor amplifiers and lasers with tapered gain regions," *Opt. Quantum Electron.*, Vol. 28, pp. 623-645, 1996.
2. A. Shima, H. Tada, K. Ono, M. Fujiwara, T. Utakouji, T. Rimura, M. Takemi, and H. Higuchi, "Highly reliable 60°C 50-mW operation of 650 nm band window-mirror laser diodes," *IEEE Photon. Technol. Lett.*, Vol. 9, pp. 413-415, 1997.

3. T. Onishi, K. Inoue, K. Onozawa, T. Takayama, and M. Yuri, "High-power and high-temperature operation of Mg-doped AlGaInP-based red laser diodes," *IEEE J. Quantum Electron.*, Vol. 40, No. 12, pp. 1634-1638, Dec. 2004.
4. B. Sumpf, M. Zorn, R. Staske, J. Fricke, P. Ressel, A. Ginolas, K. Paschke, G. Erbert, M. Weyers, and G. Tränkle, "3-W broad area lasers and 12-W bars with conversion efficiencies up to 40% at 650 nm," *IEEE J. Sel. Top. In Quantum Electron.*, Vol. 13, No. 5, pp. 1188-1193, Sept./Oct. 2007.
5. B. Sumpf, M. Zorn, J. Fricke, P. Ressel, H. Wenzel, G. Erbert, M. Weyers, and G. Tränkle, "1 W reliable operation of broad area lasers and 8 W reliable operation of 5 mm wide laser bars at 650 nm," *Proc. SPIE*, Vol. 6876, pp. 68760T, 2008.
6. B. Pezeshki, M. Hagberg, B. Lu, M. Zeleinski, S. Zou, and E. Kolev, "High power and diffraction-limited red lasers," *Proc. SPIE Conf. In-Plane Semiconductor Lasers IV*, Vol. 3947, pp. 80-90, 2000.
7. N. Linder, R. Butendeich, W. Schmid, S. Tautz, K. Streubel, C. Karnutsch, S. Ruhrländer, H. Schweizer, and F. Scholz, "900 mW continuous wave operation of AlInGaP tapered lasers and superluminescent diodes at 640 nm," *Conference on Lasers and Electro-Optics*, 2004.
8. B. Sumpf, P. Adamiec, M. Zorn, P. Froese, J. Fricke, P. Ressel, H. Wenzel, M. Weyers, G. Erbert, and G. Tränkle, "650 nm tapered lasers with 1 W maximum output power and nearly diffraction limited beam quality at 500 mW," *Proc. SPIE*, Vol. 6876, pp. 68760M, 2008.
9. M. Achtenhagen, N.V. Amarasinghe, and G.A. Evans, "High-power distributed Bragg reflector lasers operating at 1065 nm," *Electron. Lett.*, Vol. 43, pp. 755-757, 2007.
10. O. Brox, J. Wiedmann, F. Scholz, F. Bugge, J. Fricke, A. Klehr, T. Laurent, P. Ressel, H. Wenzel, G. Erbert, and G. Tränkle, "Integrated 1060 nm MOPA pump source for high-power green light emitters in display technology," *Proc. SPIE*, Vol. 6909, pp. 69091G, 2008.
11. S. Schwertfeger, J. Wiedmann, B. Sumpf, A. Klehr, F. Dittmar, A. Knauer, G. Erbert, and G. Tränkle, "7.4 W continuous-wave output power of a master oscillator power amplifier system at 1083 nm," *Electron. Lett.*, Vol. 42, pp. 346-347, 2006.
12. S. Schwertfeger, A. Klehr, G. Erbert, and G. Tränkle, "Compact hybrid master oscillator power amplifier with 3.1W cw output power at wavelength around 1061nm," *IEEE Photon. Technol. Lett.*, Vol. 16, pp. 1268-1270, 2004.
13. C. Fiebig, G. Blume, C. Kaspari, D. Feise, J. Fricke, W. Matalla, W. John, H. Wenzel, K. Paschke, and G. Erbert, "12 W high-brightness single-frequency DBR tapered diode laser," *Electron. Lett.*, Vol. 44, pp. 1253-1255, 2008.
14. H. Wenzel, K. Paschke, O. Brox, F. Bugge, J. Fricke, A. Ginolas, A. Knauer, P. Ressel, and G. Erbert, "10 W continuous-wave monolithically integrated master-oscillator power-amplifier," *Electron. Lett.*, Vol. 43, pp. 160-162, 2007.
15. L. Toikkanen, M. Dumitrescu, A. Tukianien, S. Viitala, M. Suominen, V. Erojärvi, V. Rimpilainen, R. Rönkkö, and M. Pessa, "SS-MBE grown short red wavelength range AlGaInP laser structures," *Proc. SPIE*, Vol. 5452, pp. 199-205, 2004.
16. P. Ressel, G. Erbert, U. Zeimer, K. Häusler, G. Beister, B. Sumpf, A. Klehr, and G. Tränkle, "Novel passivation process for the mirror facets of high-power semiconductor diode lasers," *IEEE Photon. Technol. Lett.*, Vol. 17, pp. 962-964, 2005.
17. P. Bienstmann, L. Vanholme, M. Ibanescu, P. Dumon, and R. Baets, "CAMFR-Cavity Modelling Framework" [Online] Available: <http://camfr.sourceforge.net/>
18. J. Fricke, H. Wenzel, M. Matalla, A. Klehr, and G. Erbert, "980 nm DBR lasers using higher order gratings defined by I-line lithography," *Semicond. Sci. Technol.*, Vol. 20, pp. 1149-1152, 2005.
19. "Optimization of SHG for high-brightness semiconductor laser diode radiation with large aberrations," *Proc. DGAO 2005*. [Online] Available: [http://www.dgao-proceedings.de/download/106/106\\_p44.pdf](http://www.dgao-proceedings.de/download/106/106_p44.pdf)

## NUSOD 2008 CONFERENCE

In September 2008, one of the BRIGHTER partners, the University of Nottingham, hosted the 8<sup>th</sup> International Conference on the Numerical Simulation of Optoelectronic Devices (NUSOD) at their University Park Campus.



### KEY FACTS AND FIGURES

- 1<sup>st</sup> – 5<sup>th</sup> September 2008
- 76 delegates from 20 countries
- 7 invited papers
- 44 regular papers
- 7 postdeadline papers
- 13 posters
- 4 short courses
- 1 software tutorial

### *Modelling of High Brightness Lasers*

One full afternoon session was devoted to the subject of modelling high-brightness lasers, a topic that is a major part of the BRIGHTER project.

#### *Presenting results from WWW.BRIGHTER.EU*

##### **“Design of 1060 nm tapered lasers with separate contacts”**

*Universidad Politécnica de Madrid, Spain & Alcatel-Thales III-V Lab, France*

##### **“Self-consistent modelling of edge-emitting GaInP/AlGaInP red lasers”**

*Universidad Politécnica de Madrid, Spain & Osram Opto Semiconductor, Germany*

##### **“Improvement of the beam quality of a broad-area diode laser using asymmetric feedback from an external cavity”**

*University of Nottingham, UK*

##### **“Numerical modelling of high power self-organising external cavity lasers”**

*University of Nottingham, UK & Laboratoire Charles Fabry de l'Institut d'Optique, France*

Further details and copies of the presentations can be found online at <http://www.nusod.org/conf08>.



**NUSOD 2008 Conference Photo**



**Welcome Reception & Poster Session**



**Group Photo – Nottingham Ghost Walk**



**The Sherriff of Nottingham & NUSOD 2008 Chairs at the Conference Dinner**

# TOPICAL MEETING AT PHOTONEX 2008

The BRIGHTER partners made a major contribution to a topical meeting on High Power Diode Lasers and Systems.

The meeting took place on 15<sup>th</sup> October 2008 in Coventry, U.K. as part of Photonex 2008. The meeting was chaired by Catrina Bryce (Univ. of Glasgow), Eric Larkins (Univ. of Nottingham) and Jim Ashe (Intense Ltd.). The meeting was sponsored by the Scottish Chapter of IEEE LEOS.

The meeting was attended by approximately 25 delegates from industry, research centres and academia. Partners from the BRIGHTER project presented four papers, one of which, a paper presented by Richard Penty (Univ. of Cambridge), was an invited talk.

The high quality of presentations on a wide range of topics, from both industrial and research perspectives, stimulated many enthusiastic discussions, making the day extremely successful.



## High Power Diode Lasers & Systems

AN EVENT AT PHOTONEX08 · [www.photonex.org](http://www.photonex.org)

Diode lasers lie at the heart of most optoelectronic systems today. Advances in the capabilities of both conventional solid state lasers and fibre lasers are being driven by improvements in power, mode structure, brightness and reliability of high power diode pump lasers.

This event highlights recent advances in diode pumped solid state lasers covering topics from advanced and novel laser pump diodes through to the applications of solid state and fibre laser systems.

### PROGRAMME

Time	Title/Speaker
09:30 - 10:00	High power diode pumped Nd:YAG technology and its application <i>Mike Mason / Powerlase</i>
10:00 - 10:15	High brightness diode laser bars and stacks using low cost micro-optics <i>Roy McBride and Denis Hall / Power Photonic</i>
10:15 - 10:45	State of the art in high brightness laser diode simulation at the University of Nottingham <i>Jun Jun Lim, Roderick MacKenzie, Lei Lang, Zhichao Zhang, Eric Larkins, Slawomir Sujecki / Photonic &amp; RF Eng. Group, University of Nottingham</i>
10:45 - 11:00	High brightness and high efficiency tapered laser at 1060 nm <i>N. Michel, M. Ruiz, M. Calligaro, M. Lecomte, O. Parillaud, M. Krakowski, H. Odriozola, J.M. Tijero and I. Esquivias / Alcatel Thales III-V Lab, France</i>
11:00 - 11:30	Coffee break
11:30 - 12:00	Diode lasers for very high power, current developments <i>Detlev Wolff / JENOPTIK Laserdiode</i>
12:00 - 12:15	By-emitter degradation analysis: Experiment and Emulation <i>Steve Bull, Christian Amuzuvi, Ruidong Xia, Jun Jun Lim, Slawomir Sujecki and Eric Larkins / Photonic and Radio Frequency Engineering Group, University of Nottingham with Jens Tomm / Max-Born Institute</i>
12:15 - 12:30	Thermally Insensitive Laser Diode Arrays for Solid State Laser Pumping <i>Andrew White, Gavin Hall and John Barr / Selex Galileo with Mark McElhinney, Prabhu Thiagarajan and Chuanshun Cao / Lasertel</i>
12:30 - 13:00	High peak power mode-locked lasers <i>Richard Penty / Centre for Photonic Systems, University of Cambridge</i>
13:00 - 14:30	Lunch
14:30 - 15:00	High efficiency and high power QCW laser bars and stacks <i>Stewart McDougall, Gianluca Bacchin, Valentine Loyo-Maldonado, John Marsh / Intense Ltd</i>
15:00 - 15:15	Power-scaling of a 1040nm microchip microlensed semiconductor disk laser <i>Nicolas Laurand, Chee Leong Lee, Erdan Gu, Stephane Calvez and Martin Dawson / Institute of Photonics, University of Strathclyde</i>
15:15 - 15:30	Solving industrial micromachining applications with fibre lasers <i>Mark Richmond / GSI Lasers</i>
15.30 - 15.45	Productivity improvements enabled by fibre laser performance versatility <i>Louise Partridge, SPI Lasers</i>

## RICH MEDIA CDs & PROJECT WEBSITE

Over the recent months, we've been busy updating our project website, [www.ist-brighter.eu](http://www.ist-brighter.eu). If you haven't checked out the site recently, then it is well worth a look at the new materials that can be found there. A wide range of new downloads are now available, including workshop presentations and technical tutorials. Many of these are available in the RichMedia CD format, which combines the presentation slides with a video of the presenter.

**Visit the BRIGHTER website at <http://www.ist-brighter.eu> for a wide range of new information and materials to download**

### More about RichMedia CDs...

RichMedia CDs are an innovative way of attending a virtual presentation, which include the transparencies of the presentation, together with synchronised video and audio of the presenter. This novel format has a clear enhanced value for presentations that are used as teaching materials and also for independent learning (as compared to the presentation slides alone). The content can be distributed not only CDs, but also online.

In a RichMedia presentation, the screen is divided in to 3 parts (see example below):

1. Presentation slides
2. Video of the presenter
3. Content and navigation panel

The video, audio and slide changes are all synchronised and a PDF file of the presentation can also be opened from the main window. A screenshot of a RichMedia presentation of a BRIGHTER tutorial is shown below.

The screenshot shows a RichMedia presentation interface with three main components:

- 1. Presentation slides:** The main content area displaying a slide titled "III V Semiconductor deposition: MOCVD". It includes a sub-heading "Chemical vapor deposition", a text box "MOCVD sources : PH<sub>3</sub>, AsH<sub>3</sub> and metalorganics based on Ga, In, Al...", an image of a reactor labeled "Reaction chamber", and a warning box "MAINTENANCE HAZARDS : sources, by products : gases and particles (dust)".
- 2. Video of the presenter:** A small video window in the top left corner showing a presenter at a desk, with a red circle '2' overlaid on it.
- 3. Content and navigation panel:** A sidebar on the bottom left containing a table of contents for "Toxicology: examples related t ...". The items listed include: Introduction, Content, Semiconductor epitaxial growth hazards, III V Semiconductor deposition: MOCVD, Cell membrane arrangement and structure, Absorption, Detoxication, Speciation, Solubility, Speciation and acute toxicity, Decreasing toxicity, As metabolism and excretion, Speciation and metabolism, Summary J. P. Buchet's studies, As toxicity, Arsenic target organs, Al compounds, Al compounds toxicity, Be toxicity, and Toxicity of gallium and indium compounds.

**See the next page for a full list of the tutorials and workshop presentations that are available online right now in the RichMedia CD format!**

## RICH MEDIA CDs & PROJECT WEBSITE

### RichMedia CDs and BRIGHTER

Over the course of the BRIGHTER project, the Consortium are developing a series of technical tutorials, each of which will be produced in the RichMedia CD format and subsequently made available on our public project website. The first of these are available online now at [www.ist-brighter.eu](http://www.ist-brighter.eu). Presentations in the RichMedia CD format are also available online now from our “Toxicology and Safety” workshop.

On the BRIGHTER website, you have four options:

1. Stream the full RichMedia presentation (slides, video, audio) from the website
2. Stream just the video recording of the presentation from the website
3. Download an *iso* image file of the RichMedia presentation from which to make your own CD
4. Download a PDF copy of the presentation slides

### 10 RichMedia Presentations Currently Available

#### Technical Training Tutorials (<http://www.ist-brighter.eu/tutorial.htm>):

1. “Toxicology and safety in III-V epitaxy” *Nicole Proust, Thales Research*
2. “Quantum dot lasers” *Johann Peter Reithmaier, University of Kassel*
3. “Mirror heating in high-power lasers” *Jens Tomm, Max Born Institute, Ignacio Esquivias, Univ. of Madrid*
4. “Efficiency of diode lasers: Basics and principles of optimisation” *Götz Erbert, Ferdinand Braun Institute*
5. “High-power high-brightness tapered diode lasers and amplifiers” *Ralf Ostendorf, Fraunhofer IAF*
6. “Major changes affecting the physical layer of optical networks” *Sébastien Bigo, Alcatel-Lucent Bell Labs*

#### From the Workshop on Safety and Toxicology ([www.ist-brighter.eu/toxicology.htm](http://www.ist-brighter.eu/toxicology.htm)):

7. “Toxicology: An Introduction” *John Duffus, The Edinburgh Centre for Toxicology*
8. “Toxicology: Examples related to As, Al, Be, Ga and In compounds” *Nicole Proust, Thales R&T*
9. “MBE Maintenance: Safety Management” *Johann Peter Reithmaier, University of Kassel*
10. “Nanomaterials and Toxicological Risk” *Allain Lombard, Allotoxconsulting*

#### COMING SOON – New Tutorials

- “By emitter degradation analysis of high-power diode laser bars” *Eric Larkins, University of Nottingham & Jens Tomm, Max Born Institute*
- “Raman amplification for telecom optical networks” *Dominique Bayart, Alcatel-Lucent Bell Labs*
- “Breaking the diffraction limit: Analysis of diode lasers by near-field scanning optical microscopy” *Jens Tomm, Max Born Institute*
- “An overview of large spot size laser structures” *Brian Corbett, Tyndall National Institute*
- “Frequency doubling and second order nonlinear optics” *Paul Michael Petersen, DTU Fotonik & Ole Bjarlin Jensen, DTU Fotonik*

For more information about BRIGHTER’s RichMedia CDs and the RichMedia format in general, please contact Jean Christophe Mielnik at Thales Research and Technology ([jean-christophe.mielnik@thalesgroup.com](mailto:jean-christophe.mielnik@thalesgroup.com)).

## SELECTED PUBLICATIONS & PRESENTATIONS

### Laser Materials, Amplifiers and Modules

- E.-M. Pavelescu, C. Gilfert, J.P. Reithmaier, A. Martín-Mínguez, I. Esquivias, "GaInAs/(Al)GaAs quantum-dot lasers with high wavelength stability," *Semicond. Sci. Technol.* Vol. 23, 085022, 2008.
- K.-H. Hasler, B. Sumpf, P. Adamiec, F. Bugge, J. Fricke, P. Ressel, H. Wenzel, G. Erbert, G. Tränkle, "5 W DBR tapered lasers emitting at 1060nm with a narrow spectral line width and a nearly diffraction limited beam quality," *IEEE Photon. Technol. Lett.* Vol. 20, pp. 1648-1650, 2008.
- E.-M. Pavelescu, C. Gilfert, J.P. Reithmaier, A. Martín-Mínguez, I. Esquivias, "High power, low threshold 1060nm InGaAs/AlGaAs QD lasers," *Int. Semiconductor Laser Conf., Sorrento, Italy*, 14<sup>th</sup>–18<sup>th</sup> Sept. 2008.
- B. Sumpf, M. Zorn, M. Maiwald, R. Staske, J. Fricke, P. Ressel, G. Erbert, M. Weyers, G. Tränkle, "5.6W broad area lasers with a vertical far field angle of 31° emitting at 670nm," *Photon. Technol. Lett.* Vol. 20, pp. 575-577, 2008.
- C.H. Kwok, R.V. Penty, I.H. White, K.-H. Hasler, B. Sumpf, G. Erbert, "Twin-contact high brightness tapered laser for high modulation efficiency high speed signal modulation," *Asia-Pacific Optical Communications Conf., Hangzhou, China*, 26<sup>th</sup>–30<sup>th</sup> Oct. 2008, Paper 7135-71.
- N. Michel, M. Ruiz, M. Calligaro, M. Lecomte, O. Parillaud, M. Krakowski, J.M.G. Tijero, I. Esquivias, "High brightness and high efficiency tapered laser at 1060nm," *High Power Laser Diodes & Systems Meeting, Coventry, U.K.*, 15<sup>th</sup> Oct. 2008.
- G. Kochem, M. Haverkamp, K. Boucke, "Frequency stabilized high brightness tapered amplifier and laser modules," *Proc. SPIE Vol. 6997, 69971A*, 2008.

### Wavelength Stabilisation and Tunable Lasers

- D. Paboeuf, G. Lucas-Leclin, N. Michel, M. Krakowski, P. Georges, "Theoretical and experimental evaluation of a wavelength-stabilized Talbot cavity with a volume Bragg grating," *Int. Semicond. Laser Conf., Sorrento, Italy*, 14<sup>th</sup>–18<sup>th</sup> Sept. 2008.
- G. Lucas-Leclin, D. Paboeuf, P. Georges, J. Holm, P. Andersen, B. Sumpf, G. Erbert, "Wavelength stabilization of extended-cavity tapered lasers with volume Bragg grating," *Appl. Phys. B* Vol. 91, pp. 493-498, 2008.
- D. Paboeuf, G. Lucas-Leclin, P. Georges, B. Sumpf, G. Erbert, C. Varona, P. Loiseau, G. Aka, B. Ferrand, "Blue laser emission by intracavity SHG in Nd:ASL pumped by a tapered amplifier laser diode stabilized by a volume Bragg grating," *Appl. Phys. B* Vol. 92, pp. 189-193, 2008.
- R. Bohdan, A. Bercha, W. Trzeciakowski, F. Dybala, B. Piechal, M. Bou Sanayeh, M. Reufer, P. Brick, "Yellow AlGaInP/InGaP laser diodes achieved by pressure and temperature tuning," *J. Appl. Phys.* Vol. 104, 063105, 2008.
- F. Dybala, A. Bercha, B. Piechal, W. Trzeciakowski, R. Bohdan, M. Mrozowicz, A. Klehr, P. Ressel, H. Wenzel, B. Sumpf, G. Erbert, "Pressure and temperature tuning of external cavity InGaAsP laser diode," *Semicond. Sci. Technol.* Vol. 23, 125012, 2008.
- D. Vijayakumar, O.B. Jensen, B. Thestrup, "High power NIR laser bar with improved beam quality," *European Semicond. Laser Workshop, Eindhoven, Netherlands*, 19<sup>th</sup>–20<sup>th</sup> Sept. 2008.

### Diode Laser Physics, Degradation and Reliability

- M. Ziegler, R. Pomraenke, M. Felger, J.W. Tomm, P. Vasa, C. Lienau, M. Bou Sanayeh, A. Gomez-Iglesias, M. Reufer, F. Bugge, G. Erbert, "Infrared emission from the substrate of GaAs-based semiconductor lasers," *Appl. Phys. Lett.* Vol. 93, 041101, 2008.
- S. Bull, J.W. Tomm, E.C. Larkins, "Identification of degradation mechanisms in high-power laser bars using by-emitter degradation studies," *J. Mat. Sci.: Mat. Electron.* Vol. 19, pp. S145–S149, 2008.
- M. Ziegler, V. Talalaev, J.W. Tomm, T. Elsässer, B. Sumpf, G. Erbert, "Surface recombination and facet heating in high-power diode lasers," *Appl. Phys. Lett.* Vol. 92, 203506, 2008.
- S. Bull, C.K. Amuzuvi, J.W. Tomm, R. Xia, J.J. Lim, S. Sujecki, E.C. Larkins, "By-emitter degradation analysis: Experiment and Emulation," *High Power Laser Diodes & Systems Meeting, Coventry, U.K.*, 15<sup>th</sup> Oct. 2008.
- T. Westphalen, M. Leers, C. Scholz, K. Boucke, "Emitter resolved analysis of packaged laser bars," *Proc. SPIE Vol. 6876, 68760O*, 2008.
- M. Ziegler, J.W. Tomm, T. Elsaesser, C. Monte, J. Hollandt, H. Kissel, J. Biesenbach, "Cavity-enhanced thermal emission from semiconductor lasers," *J. Appl. Phys.* Vol. 103, 104508, 2008.

### Laser Diode Design, Modelling and Optimisation

- H. Odriozola, J.M.G. Tijero, I. Esquivias, L. Borrueal, A. Martín-Mínguez, N. Michel, M. Calligaro, M. Lecomte, O. Parillaud, M. Krakowski, "Design of 1060nm tapered lasers with separate contacts," *Numerical Simulation of Optoelectronic Devices Conf., Nottingham, U.K.*, 1<sup>st</sup>–5<sup>th</sup> Sept. 2008, Paper TuC2.
- J.M.G. Tijero, H. Odriozola, I. Esquivias, A. Martín-Mínguez, P. Brick, M. Reufer, M. Bou Sanayeh, A. Gomez-Iglesias, N. Linder, "Analysis of the leakage current of GaInP/AlGaInP high power lasers with a self-consistent simulation model," *Numerical Simulation of Optoelectronic Devices Conf., Nottingham, U.K.*, 1<sup>st</sup>–5<sup>th</sup> Sept. 2008, Paper TuC5.
- Z. Zhang, G. Pauliat, J.J. Lim, P.J. Bream, N. Dubreuil, A.J. Kent, E.C. Larkins, S. Sujecki, "Numerical modelling of high-power self-organizing external cavity lasers," *Numerical Simulation of Optoelectronic Devices Conf., Nottingham, U.K.*, 1<sup>st</sup>–5<sup>th</sup> Sept. 2008, Paper MP18.
- L. Lang, J.J. Lim, S. Sujecki, E.C. Larkins, "Improvement of the beam quality of a broad-area diode laser using asymmetric feedback from external cavity," *Numerical Simulation of Optoelectronic Devices Conf., Nottingham, U.K.*, 1<sup>st</sup>–5<sup>th</sup> Sept. 2008, Paper ThPD7.
- H. Odriozola, J.M.G. Tijero, L. Borrueal, I. Esquivias, H. Wenzel, F. Dittmar, K. Paschke, B. Sumpf, G. Erbert, "Beam properties of 980nm tapered lasers with separate contacts: Experiments and simulations," *J. Quantum Electron.* (in press), Nov. 2008.
- J.J. Lim, S. Sujecki, L. Lang, Z. Zhang, D. Paboeuf, G. Pauliat, G. Lucas-Leclin, P. Georges, R. MacKenzie, P. Bream, S. Bull, K.-H. Hasler, B. Sumpf, H. Wenzel, G. Erbert, B. Thestrup, P.M. Petersen, N. Michel, M. Krakowski, E.C. Larkins, "Design and simulation of next-generation high-power, high-brightness laser diodes," (invited) submitted to *J. Select. Topics Quantum Electron.*, Nov. 2008.

PROJECT e-NEWSLETTERS

Don't miss the next WWW.BRIGHTER.EU e-Newsletter!

Look out for the following in Edition 5 in March 2009:

- Partner profiles – *Biolitec AG, Tyndall National Institute, Thales Research and Technology, Institute of High Pressure Physics (UNIPRESS)*
- “WDM amplification” – *Alcatel-Lucent Bell Labs*
- “Wavelength tuning of laser diodes by hydrostatic pressure” – *UNIPRESS*
- “Red high power lasers” – *OSRAM Opto Semiconductor*
- “High-brightness laser modules” – *Fraunhofer Institute for Laser Technology*

e-Newsletter n°5

March 2009  
Available at [www.ist-brighter.eu](http://www.ist-brighter.eu)

World Wide Welfare: High-Brightness Semiconductor Lasers for Generic Use

WWW.BRIGHTER.EU is an integrated project supported by the European Commission's Information Society Technologies programme

CONTENT

Greetings from the Project Coordinator	2
<b>PROJECT NEWS</b>	
Latest Achievements	3
Partner Presentations	6

e-Newsletter Back Issues

If you missed either of our first 3 e-Newsletters, or would like to see our 3 e-Newsletters from the earlier WWW.BRIGHTER.EU project, please visit our website at <http://www.ist-brighter.eu>, where .pdf copies of all published e-Newsletters can be downloaded.

Some highlights of previous e-Newsletters!

Applications Articles

- Diode lasers for display applications
- Optical wireless communication systems
- Raman amplification
- Pumping of fibre lasers

.....and many more

Technical Papers

- Spectral modelling of high-brightness laser diodes
- Overgrowth free high-power single mode lasers
- By-emitter degradation analysis of high-power laser bars
- Pressure and temperature tuning of laser diodes

.....and many more

## CALENDAR OF EVENTS

The calendar below lists some events in the first half of 2009 at which the Consortium will be represented.

**24<sup>th</sup> – 29<sup>th</sup> January**

**SPIE Photonics West, San Jose, CA, U.S.A**

**22<sup>nd</sup> – 26<sup>th</sup> March**

**Optical Fiber Communication Conference (OFC), San Diego, CA, U.S.A**

**6<sup>th</sup> – 8<sup>th</sup> April**

**Semiconductor and Integrated Optoelectronics Conference (SIOE), Cardiff, Wales, U.K.**

**13<sup>th</sup> – 17<sup>th</sup> April**

**Materials Research Society (MRS) – Spring Meeting, San Francisco, CA, U.S.A**

**31<sup>st</sup> May – 5<sup>th</sup> June**

**Conference on Lasers and Electro-Optics (CLEO), Baltimore, MD, USA**

**8<sup>th</sup> – 12<sup>th</sup> June**

**European Materials Research Society (EMRS) – Spring Meeting, Strasbourg, France**

**6<sup>th</sup> – 13<sup>th</sup> June**

**International Graduate Summer School on Biophotonics, Ven, Sweden**

**14<sup>th</sup>– 19<sup>th</sup> June**

**European Conference on Lasers and Electro-Optics (CLEO-Europe), Munich, Germany**

**14<sup>th</sup> – 18<sup>th</sup> June**

**European Conferences on Biomedical Optics (ECBO), Munich, Germany**

**15<sup>th</sup> – 18<sup>th</sup> June**

**LASER 2009 – World of Photonics Exhibition, Munich, Germany**

## ICT 2008 EVENT

*Europe's biggest ICT research event*

**Lyon, 25<sup>th</sup> – 27<sup>th</sup> November 2008**

The WWW.BRIGHTER.EU Consortium and Project Partner Biolitec will be at ICT 2008, Europe's biggest ICT research event, later this month in Lyon.



**Visit BRIGHTER at Stand L01  
in ICT for Wellbeing - Village L**

**Visit Biolitec at Stand  
C07 in the SME Village**

